THE POTENTIAL ROLE OF NODAL IN ZEBRAFISH TESTIS

RIDDHI JANI

A THESIS SUBMITTED TO
THE FACULTY OF GRADUATE STUDIES
IN PARTIAL FULFILMENT OF THE REQUIREMENTS
FOR THE DEGREE OF
MASTER OF SCIENCE

GRADUATE PROGRAM IN BIOLOGY
YORK UNIVERSITY
TORONTO, CANADA

DECEMBER 2025

ABSTRACT

The TGF-β superfamily regulates a range of physiological processes, including development, cell differentiation, and reproduction. While several TGF-β members are well characterized in adult gonadal function, the role of Nodal, a key regulator of early embryogenesis, remains poorly understood in reproduction. This project investigated the potential involvement of Nodal in zebrafish testis physiology. Analysis of offspring from heterozygous *ndr1* mutant crosses revealed no significant changes in sex ratio compared to wild-type fish. Gene expression profiling indicated that *ndr1* is highly expressed in 9-month-old testis. *Ex vivo* testis culture with recombinant human Nodal induced time-dependent upregulation of the Nodal inhibitor *lft1*. RNA-seq analysis of Nodal-treated testis identified modest but coordinated changes in pathways associated with reproductive processes, sperm–egg interactions, cellular organization, and immune response. These findings provide new insight into Nodal pathway activity in the zebrafish testis and lay groundwork for future studies on its role in vertebrate reproductive biology.

ACKNOWLEDGEMENTS

First and foremost, I would like to sincerely thank my supervisor, Dr. Chun Peng, for her invaluable guidance, support, and encouragement throughout this project. Her expertise and mentorship were instrumental in shaping both the scientific direction of this work and my growth as a researcher.

I am also grateful to my advisor, Dr. Raymond Kwong, for his thoughtful feedback and insightful suggestions, which helped refine the project.

A huge thank you to the zebrafish facility staff, particularly Janet Fleites Medina and Veronica Scavo, for their guidance, technical support, and dedication to maintaining the health and wellbeing of the animals used in this study. My appreciation also goes to Claire Yu, whose expertise in RNA-seq analysis and statistical guidance greatly strengthened the quality and interpretation of the data.

Many thanks to my fellow fish people, Gagan Sidhu and Sajid Alvi, for the long experimental days that somehow turned into great conversations about movies, music, and everything in between. Those coffee runs were less about caffeine and more about sanity, and I couldn't have asked for better company. I am also thankful to Tobi Agbede, Sihat Salam, and Rufei Yan for the occasional much-needed comic relief between PCR runs. And to my lab mates, thank you for the teamwork, advice, and unspoken understanding that comes with surviving research together.

Finally, to my family: thank you for your constant love, patience, and encouragement over these past few years.

TABLE OF CONTENTS

LIST OF TABLES

CHAPTER 2

CHAPTER 3

LIST OF FIGURES

CHAPTER 1

CHAPTER 3

APPENDICES

LIST OF ABBREVIATIONS

11-KT	11-Ketotestosterone
AMH	Anti-Müllerian Hormone
BMP	Bone Morphogenetic Protein
CG	Cortical Granule
CRF	Corticotropin-releasing factor
DPF	Days Post-Fertilization
FPKM	Fragments Per Kilobase of Transcript per Million Mapped Reads
GDF	Growth and Differentiation Factor
GO	Gene Ontology
HPG	Hypothalamic–Pituitary–Gonadal (Axis)
HPI	Hypothalamic–Pituitary–Interrenal (Axis)
MAPK	Mitogen-Activated Protein Kinase
MS-222	Tricaine Methanesulfonate
ndr	Nodal-related
PCA	Principal Component Analysis
padj	Adjusted p-value
PGCs	Primordial Germ Cells
rhNodal	Recombinant Human Nodal
R-Smad	Receptor-Regulated SMAD Protein
SSC	Spermatogonial Stem Cell
SVA	Surrogate Variable Analysis
TGF-β	Transforming Growth Factor Beta

CHAPTER 1

INTRODUCTION

1.1. Zebrafish as a model organism

Zebrafish (*Danio rerio*) have emerged as a prominent model organism in biomedical research due to several key advantages. They have a fully sequenced genome, with 70% of human genes related to genes found in zebrafish [1], making them a valuable system for studying genetic and physiological processes relevant to human health. Zebrafish embryos are transparent, allowing direct visualization of developmental processes and internal structures without the need for dissection [2,3]. Embryos also exhibit rapid development, with most organs forming within the first few days of life, which allows researchers to track changes in embryo development from fertilization. Zebrafish can produce large numbers of offspring and reach sexual maturity in about three months, which is especially beneficial for large-scale studies [2]. Additionally, zebrafish research has been enhanced by gene editing tools. Techniques such as CRISPR, transgenesis, and gene knockouts enable precise genetic modifications to study gene function and disease mechanisms [4]. Because their genetic pathways are highly conserved with humans, zebrafish models have been used to study human diseases, including cardiovascular disorders [5], and neurodegenerative conditions [6]. Collectively, these attributes make zebrafish versatile and powerful model organisms for studying vertebrate development, genetics, and disease mechanisms.

1.2. Zebrafish reproduction

1.2.1. Germ cell development

Zebrafish germ cell development begins shortly after fertilization, with primordial germ cell (PGC) migration and proliferation occurring within the first few days post-fertilization (dpf). Around 5 dpf the somatic gonad becomes visible; then from 7–10 dpf both somatic gonad cells and germ cells start proliferating. By 12 dpf the gonad remains undifferentiated and bi-potential, expressing both male- and female-associated genes. Between 13–14 dpf early-stage oocytes (gonocytes) appear, which give the gonad an ovary-like appearance, yet it is still bi-potential [7]. The number of germ cells at this stage matters: higher germ-cell numbers favour female fate, whereas lower numbers skew toward male fate [8]. Sexual differentiation becomes evident around 20–25 dpf: in the undifferentiated gonad one observes stage 1A and early stage 1B oocytes [7,9]. In fish destined to become male, these oocytes undergo apoptosis; in female-fated fish they continue along meiosis. Between 25 and 45 dpf, future males experience apoptosis of the juvenile ovaries and subsequent transformation into testis, while females proceed with ovarian development. The timing of this transition varies among individuals. Ovarian differentiation in females becomes pronounced by around 60 dpf with the growth of oocytes and adults reach sexual maturity by approximately 90 dpf [8].

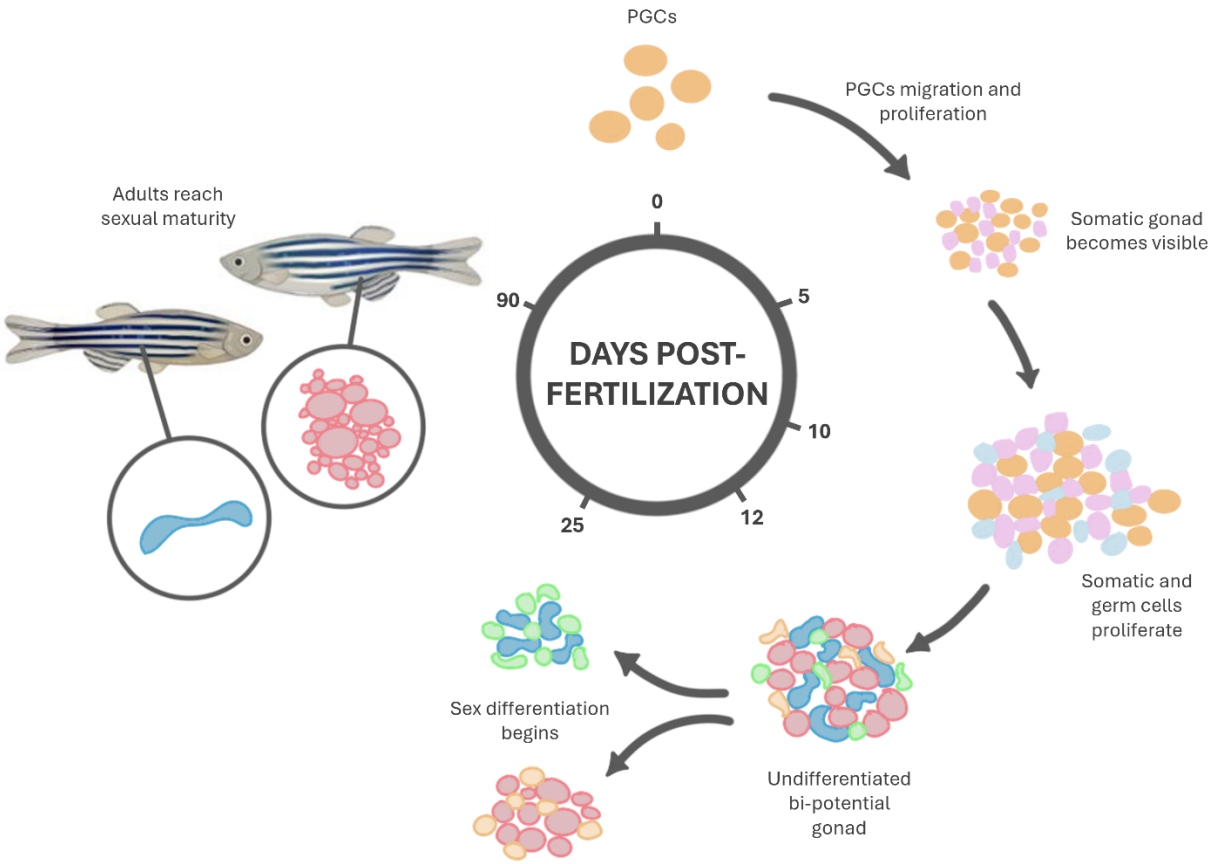

Figure 1: Zebrafish germ cell development. Shortly after fertilization (0–1 dpf), PGCs are specified and begin to form. Between 1–5 dpf, PGCs migrate and proliferate toward the future gonad site. By around 5 dpf, the somatic gonad becomes visible as clusters of somatic cells. At 7–10 dpf, both somatic gonad cells and germ cells proliferate. By 12 dpf, the gonad is undifferentiated and bi-potential, expressing both male- and female-associated genes. Early-stage oocytes appear at 13–14 dpf, and germ cell number influences sex fate, with higher counts favoring female development. Sexual differentiation begins between 20–25 dpf, when male-fated oocytes undergo apoptosis while female-fated oocytes continue meiosis. From 25–45 dpf, juvenile ovaries in future males degenerate and transform into testis, while female ovarian development continues. By around 60 dpf, ovarian differentiation is pronounced with marked oocyte growth. Adults have fully formed gonads and reach sexual maturity by 90 dpf. This timeline captures key stages and cellular behaviors underlying zebrafish germ cell development and sex differentiation. Illustration created on Autodesk Sketchbook Pro (adult zebrafish assets from BioRender).

1.2.2. Sex determination and differentiation

Sex determination in zebrafish is governed by a complex polygenic system rather than a single dominant master gene. Unlike some wild zebrafish populations, which exhibit a ZZ/WZ sex chromosome system, most laboratory zebrafish strains lack morphologically distinct sex chromosomes, and their sexual fate is influenced by the combined action of autosomal genes, germ cell number, and environmental cues.

Several key genes play essential roles in sex differentiation and determination in zebrafish, organizing the direction of gonadal fate through a network of molecular actions. Genes such as *dnd*, *vasa*, *nanos2*, *nanos3*, and *dazl* regulate primordial germ cell migration, specification, and stem cell maintenance, establishing the foundation for later sexual development [7]. Cell cycle regulators like *cdk21* influence germ cell proliferation , while the transcription factor *dmrt1* and anti-Müllerian hormone (*amh*) are crucial for guiding male differentiation from a bi-potential gonad [10,11]. In the female pathway, aromatase encoded by *cyp19a1a* dictates the conversion of androgen precursors into estrogen and promoting ovarian fate [12]. Emerging modulators like *miR214* and *gsdf* highlight the involvement of microRNA and teleost-specific genes in sex determination through post-transcriptional regulation [13]. Altogether, these genes coordinate the sex differentiation process in zebrafish prior to overt testicular or ovarian development, with further plasticity shaped by epigenetic and environmental inputs.

1.2.3. Fertilization in zebrafish

Mature, capacitated sperm are released into the lumen of the testis and ultimately expelled into the water during spawning events, where external fertilization occurs. Fertilization success is

influenced by sperm motility, density, and viability, all of which are regulated by hormonal and paracrine signaling from the testis [14]. In zebrafish, the sperm lack a typical acrosome (there is no classical “acrosome reaction” as seen in mammals). The sperm swim to the micropyle — a narrow channel in the egg envelope — through which it binds to the egg’s plasma membrane [15]. The entry of sperm triggers activation of the egg, marked by a dramatic rise in intracellular calcium (Ca^{2+}), which is essential for transforming the haploid gametes into a fertilization-competent zygote. It was recently reported that zebrafish eggs autonomously initiate a protease-activated receptor 2-triggered calcium elevation that spreads in a wave across the egg [16].

With a rise in Ca^{2+}, the cortical reaction begins with the exocytosis of cortical granules (CGs) from the egg. This process causes the elevation and modification of the chorion (egg envelope), which creates a fertilization envelope that acts as a physical and chemical barrier to prevent entry of additional sperm. The translocation of CGs to the egg cortex during oogenesis is regulated by maternal-effect genes such as *krang*, over easy (*ovy*), and *p33bjta*, and involves *Rab11* and an actin-based network for proper CG positioning and exocytosis [17]. Following the cortical reaction, the male and female pronuclei migrate toward each other and fuse, forming a diploid zygote nucleus, thus completing fertilization and resulting in a fertilized egg ready for embryonic development [16].

1.3. Zebrafish testis development

1.3.1. Spermatogenesis

Spermatogenesis in zebrafish is a continuous, cystic process that begins with spermatogonial stem cells (SSCs) residing in a specialized niche surrounded by Sertoli cells, which support both their self-renewal and differentiation [18]. These SSCs differentiate into type A spermatogonia, which proliferate mitotically within a Sertoli cell cyst, forming a clonal syncytium before becoming type B spermatogonia that undergo approximately nine mitotic divisions [19]. The germ cells then enter meiosis and undergo two rounds of cell division, which produces secondary spermatocytes and then spermatids. Following meiosis, spermatids undergo spermiogenesis where they undergo nuclear condensation, organelle elimination, and flagellum formation to become mature spermatozoa within the same cyst. Finally, the Sertoli cell cyst opens to release mature spermatozoa into the lumen of the seminiferous tubules, making them available for fertilization [18]. This entire process, from the initiation of mitosis to the formation of spermatozoa, takes approximately six days in zebrafish and involves a high degree of Sertoli cell support and a significant, though regulated, loss of germ cells [18].

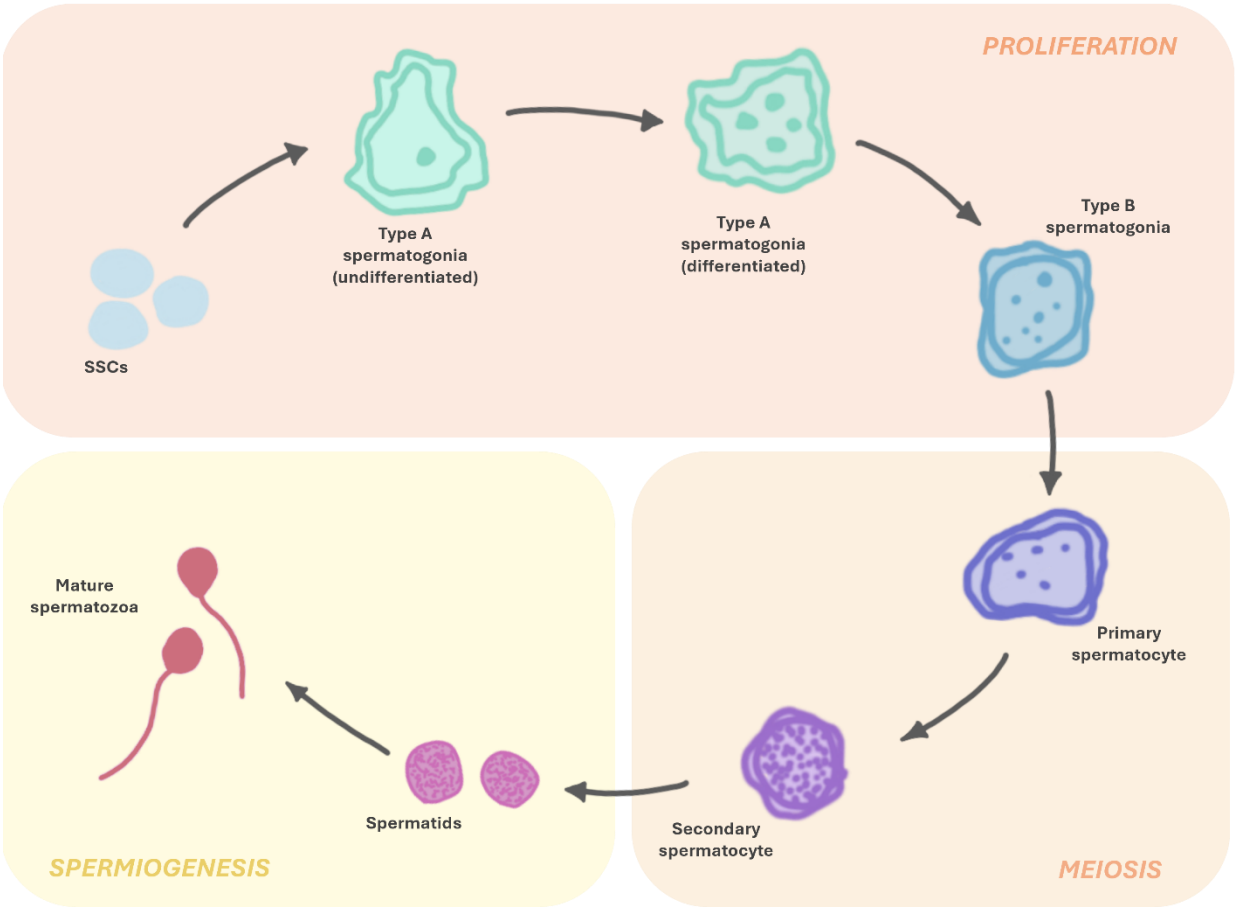

Figure 2: Spermatogenesis in zebrafish. Spermatogonial stem cells (SSCs) in their specialized Sertoli cell niche self-renew or differentiate into undifferentiated type A spermatogonia, which proliferate mitotically within Sertoli cell cysts. These cells then progress to differentiated type A spermatogonia, followed by multiple rounds of mitotic divisions as type B spermatogonia. Subsequently, type B spermatogonia enter meiosis I as primary spermatocytes and rapidly proceed through meiosis II as secondary spermatocytes, giving rise to haploid spermatids. Spermatids undergo morphological transformation during spermiogenesis, including nuclear condensation and flagellum formation, to become mature spermatozoa. Mature spermatozoa are then released into the lumen of seminiferous tubules upon breakdown of the Sertoli cyst. Supporting cell types such as Sertoli cells, Leydig cells, and immune cells aid and regulate this complex process. Illustration created on Autodesk Sketchbook Pro; based on information from Schulz et al. (2018) and Leal et al. (2009). Cell sizes are not to scale.

1.3.2. Regulation of testis development

Testis formation in zebrafish begins with the formation of a bipotential juvenile ovary, which can develop into either ovaries or testis. This differentiation process is influenced by several factors, including the number of germ cells present. Research has shown that a complete absence of germ cells leads to sterile males, indicating that a threshold number of primordial germ cells is crucial for normal testis development and function [10,20]. Some key genes involved in testis development include *dmrt1*, *amh*, and *ar* [20]. The *dmrt1* gene is particularly crucial as it promotes testis differentiation even in the absence of normal androgen signaling, as seen in *cyp17a1*-deficient zebrafish, where androgen and estrogen synthesis is compromised [10,21]. Additionally, insulin-like 3, which is produced by Leydig cells, affects spermatogenic cells directly and through signaling pathways such as retinoic acid and peroxisome proliferator-activated receptor gamma, which are involved in the differentiation of spermatogonia [22].

1.3.3. Regulation of testis function

Beyond initial spermatogenesis, the adult zebrafish testis maintains continuous sperm production through the ongoing proliferation of spermatogonial stem cells within cysts, supported by Sertoli cells [23]. Leydig cells produce androgens, primarily 11-ketotestosterone (11-KT), which regulate both Sertoli cell function and germ cell differentiation [24]. Paracrine factors, including members of the TGF-β superfamily such as activins, inhibins, AMH, and Gsdf, modulate these processes, ensuring coordinated spermatogenesis and testicular homeostasis [25–27].

In laboratory environments, it is well accepted that a photoperiod of 10-hour light and 14-hour dark and a temperature of 28°C are optimal conditions for efficient zebrafish reproduction [14].

Deviations from these conditions have been shown to interfere with reproduction as spermatogenic activity and steroid hormone production are regulated by both environmental factors and endocrine signaling. Photoperiod and temperature act as external cues that synchronize reproductive cycles with optimal conditions for spawning, influencing the timing and rate of spermatogonial proliferation as well as Leydig cell steroidogenesis. For example, researchers found that in a high temperature environment, the *trpv4* gene encoding a temperature-sensitive ion channel in the Leydig cells was upregulated, steroid synthesis was reduced in Leydig cells, and sperm motility was downregulated [28].

Internally, the hypothalamic-pituitary-gonadal (HPG) axis mediates hormonal control: gonadotropin-releasing hormone (GnRH) from the hypothalamus stimulates the pituitary to secrete follicle-stimulating hormone (FSH) and luteinizing hormone (LH), which act on Sertoli and Leydig cells, respectively. FSH promotes Sertoli cell support of germ cells and paracrine signaling, while LH stimulates androgen production in the Leydig cells, primarily 11-ketotestosterone. 11-KT is synthesized from testosterone through the sequential actions of Cyp11c1, which hydroxylates testosterone to 11β-hydroxytestosterone, and Hsd11b2, which converts it to 11-KT [14,29]. Unlike mammals, in which testosterone is the key androgen that maintains spermatogenesis, the main circulating androgen in teleost fish is 11-KT, which has been reported to be involved in spermatogonial proliferation, germ cell maturation, and the development of secondary sexual characteristics [30,31].

Emerging evidence suggests an overlap between the HPG and hypothalamus–pituitary–interrenal (HPI) axes. This is partly due to the notion that synthesis of cortisol (a key player in the HPI axis) depends on the coordinated action of key enzymes including steroidogenic acute regulatory

protein (*star*), cytochrome P450 11a2 (*cyp11a2*), and 11β-hydroxysteroid dehydrogenase type 2 (*hsd11b2*), which are also expressed within the gonads where they aid in steroid hormone production [32]. The overlap is demonstrated in studies where a knockout in the gene *cyp11c1* (which is required for 11-KT and cortisol synthesis) led to delayed ovary-to-testis transition and defective spermatogenesis. Specifically, in *cyp11c1*$^{-/-}$ males, expression of Leydig-cell/Sertoli-cell genes (e.g., *insl3*, *cyp17a1*, *amh*) was significantly decreased, which then caused down-regulation of the male germ-cell regulator *dmrt1* and led to insufficient spermatogenesis [31]. Within the testis, cortisol reportedly acts through glucocorticoid receptor isoforms (*gr*α and *gr*β) expressed in Sertoli, Leydig, and germ cells, where it stimulates spermatogonial proliferation, meiosis, and spermiogenesis independently of androgens [33]. Another study showed that sex steroids can modulate the HPI axis: estradiol suppressed cortisol responses and corticotropin-releasing factor (CRF) expression in males, while 11-KT increased cortisol in resting males and stressed females without affecting CRF or cortisol synthesis *in vitro* [34].

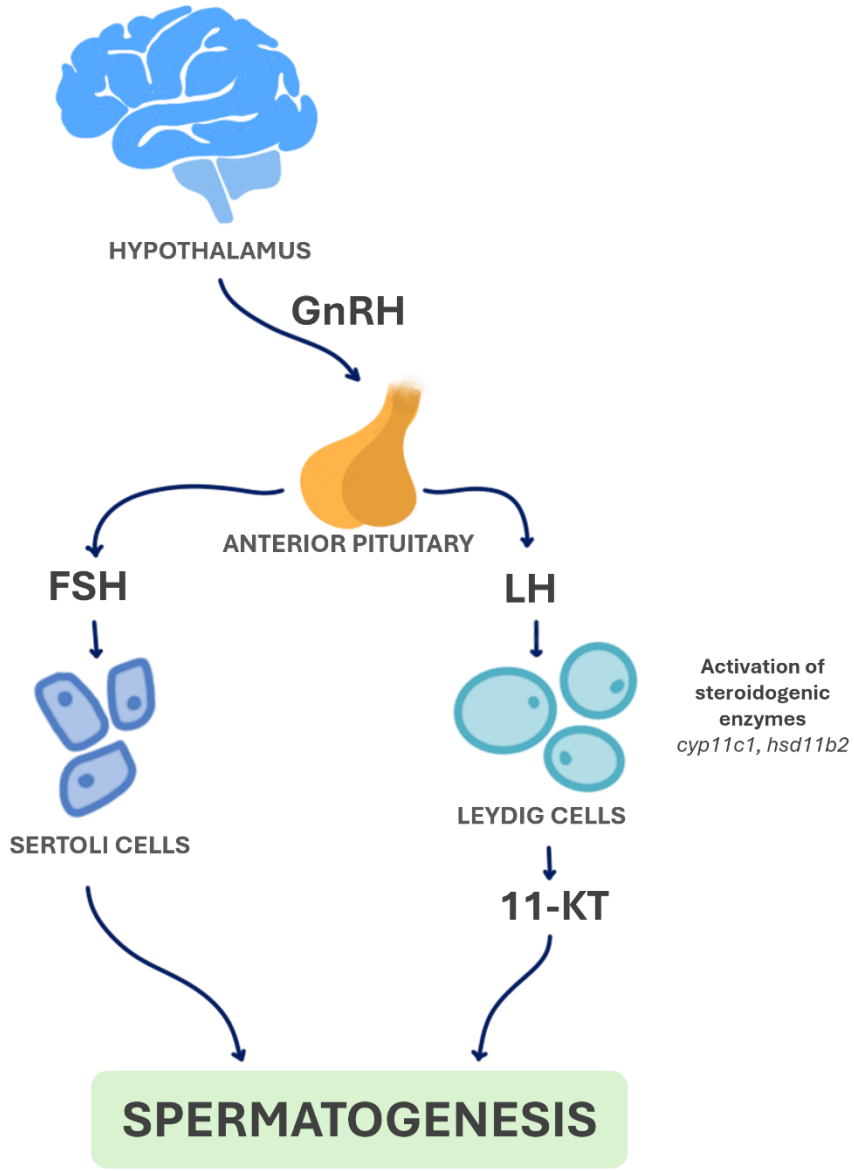

Figure 3: Regulation of zebrafish testis function via the HPG axis. Schematic representation of the hypothalamic–pituitary–gonadal axis. The HPG axis begins with hypothalamic secretion of GnRH, which triggers the release of gonadotropins LH and FSH from the anterior pituitary. FSH acts on Sertoli cells to support spermatogenesis, while LH stimulates Leydig cells to produce androgens (testosterone, which is converted to 11-KT, the main circulatory androgen), which promote spermatogenesis. Illustration created on Autodesk Sketchbook Pro.

1.4. The TGF-β superfamily

1.4.1. Roles in reproduction

The transforming growth factor-β (TGF-β) superfamily consists of structurally similar proteins that play important roles in various physiological activities, including reproduction. This superfamily encompasses various subfamilies, such as TGF-βs, activins, inhibins, bone morphogenetic proteins (BMPs), growth differentiation factors (GDFs), AMH, and Nodal.

Many members of this superfamily have documented roles in regulatory reproductive processes in both males and females. For instance, TGF-β1 and BMP-15 inhibit oocyte maturation in zebrafish [35], while activin has been shown to enhance the process [36]. TGF-βs, BMP-15, activins, and GDF9 influence follicle growth, steroidogenesis, oocyte maturation, and ovulation in mammalian ovaries [37]. Studies also revealed that a loss of activin/inhibin βA subunits impaired female follicle development [26]. TGF-β superfamily ligands are also involved in regulating somatic–germ cell interactions and spermatogenesis. For example, activin A promotes Sertoli-cell proliferation and germ-cell differentiation [38], while inhibin antagonizes activin's effect and modulates FSH release and paracrine gonadal signals [39]. AMH, which is secreted by Sertoli cells in male embryos, is essential for the regression of Müllerian ducts during male embryonic development, preventing the formation of female reproductive structures [40]. BMP4, which is expressed in the Leydig cells, inhibits the differentiation of stem/progenitor Leydig cells into adult Leydig cells by suppressing steroidogenesis [41]. In zebrafish, the Sertoli-cell-expressed ligand Gsdf is required to maintain proper germ-cell numbers and support spermatogonial maintenance [25].

1.4.2. TGF-β signaling pathway

TGF-β superfamily members initiate signaling through a conserved mechanism involving serine/threonine kinase receptors and intracellular Smad proteins. The process begins with TGF-β ligands binding to type I and type II serine/threonine kinase receptors [42]. Type II receptors phosphorylate type I receptors, which then phosphorylate receptor-regulated Smad proteins (R-Smads), triggering the Smad-signaling cascade [43]. R-Smads that have been phosphorylated by type I receptors form a complex with Smad4, which then translocates to the nucleus and interacts with transcription factors to control gene expression [42]. Beyond the canonical Smad-signaling pathway, TGF-β superfamily ligands can also activate non-Smad pathways, such as mitogen-activated protein kinases (MAPKs) [44] and the Akt/PKB pathway [45], thereby diversifying their cellular effects.

1.5. Nodal

1.5.1. Nodal's crucial role during embryogenesis

Nodal signaling is crucial during embryonic development, influencing processes such as mesoderm and endoderm formation, neural patterning, and the establishment of left-right asymmetry [46–48]. In zebrafish, three Nodal homologs, called nodal-related (ndr), exist: squint (*ndr1*), cyclops (*ndr2*), and southpaw (*ndr3*). During gastrulation, *ndr1* and *ndr2* are involved in meso-endoderm specification, whereas *ndr3*, though not expressed during gastrulation, is essential for the correct positioning and asymmetrical development of visceral organs, including the heart and brain structures [49,50]. The formation of meso-endodermal tissues is important for proper embryo development and loss of Nodal signaling can lead to morphological defects in

embryos, such as cyclopia and severe body axis curvature. For instance, a loss of *ndr1* and *ndr2* causes severe developmental defects in the developing embryo: double mutants lack most meso-endoderm-derived structures such as the notochord, trunk, heart, blood, and gut, whereas single mutants exhibit dorsal defects, including cyclopia and craniofacial malformations [46,51].

1.5.2. Canonical Nodal signaling pathway

During the mid-to-late blastula stage (3–4 hpf) of embryogenesis in zebrafish, Nodal expression is initiated downstream of Wnt/β-catenin signaling, with β-catenin localized dorsally in the yolk cell activating transcription of *ndr1* and *ndr2*. Both genes are initially expressed at the blastodermal margin, which comprises cells destined to become mesoderm and endoderm. Maternal factors such as Eomesa broadly activate *ndr1* and *ndr2* expression along the blastoderm margin, while maternal Hwa-activated β-catenin signaling induces *ndr1* expression more specifically on the dorsal margin. Functionally, *ndr1* and *ndr2* drive meso-endoderm induction during blastula and gastrula stages (5–10 hpf) [52]. Later in development, after gastrulation, *ndr3* becomes expressed in the left-right organizer (known as Kupffer's Vesicle) and in the left lateral plate mesoderm, where it governs left-right axis formation and organ laterality [53]. Altogether, *ndr1* and *ndr2* orchestrate early meso-endodermal patterning, while *ndr3* regulates subsequent left-right asymmetry, marking distinct waves of Nodal gene activity in zebrafish embryogenesis [54].

The ligands are secreted as precursors that must dimerize and be proteolytically cleaved by subtilisin-like proteases, such as Furin and Pace4, to become active. Active dimers bind type I and type II activin-like kinase receptors (ALK4/ActRIIB) [48], and for effective signal transduction, Nodal ligands require specific co-receptors. EGF-CFC proteins like mammalian Cripto (also known as

TDGF1) and zebrafish One-eyed pinhead (Oep) are essential co-receptors that facilitate Nodal's interaction with its primary receptors by enhancing Nodal's binding affinity to its receptors and promoting downstream signaling [55,56]. Receptor activation phosphorylates Smad2 and Smad3, which form a complex with Smad4 and translocate to the nucleus. Nuclear Smads interact with transcription factors, including FOXH1 and Mixer, to induce target genes such as *goosecoid* and the Nodal inhibitors *lefty1/2* [48]. While it is well documented that Nodal induces its own expression via positive feedback loop, it also induces the expression of Lefty, a subclass of TGF-β proteins and a known inhibitor of Nodal [48,49]. Lefty proteins (encoded by *lft1* and *lft2* in zebrafish) act as extracellular antagonists of Nodal signaling, wherein they inhibit Nodal activity by competing for binding to activin receptors and interfering with the interaction between Nodal and its co-receptors [57].

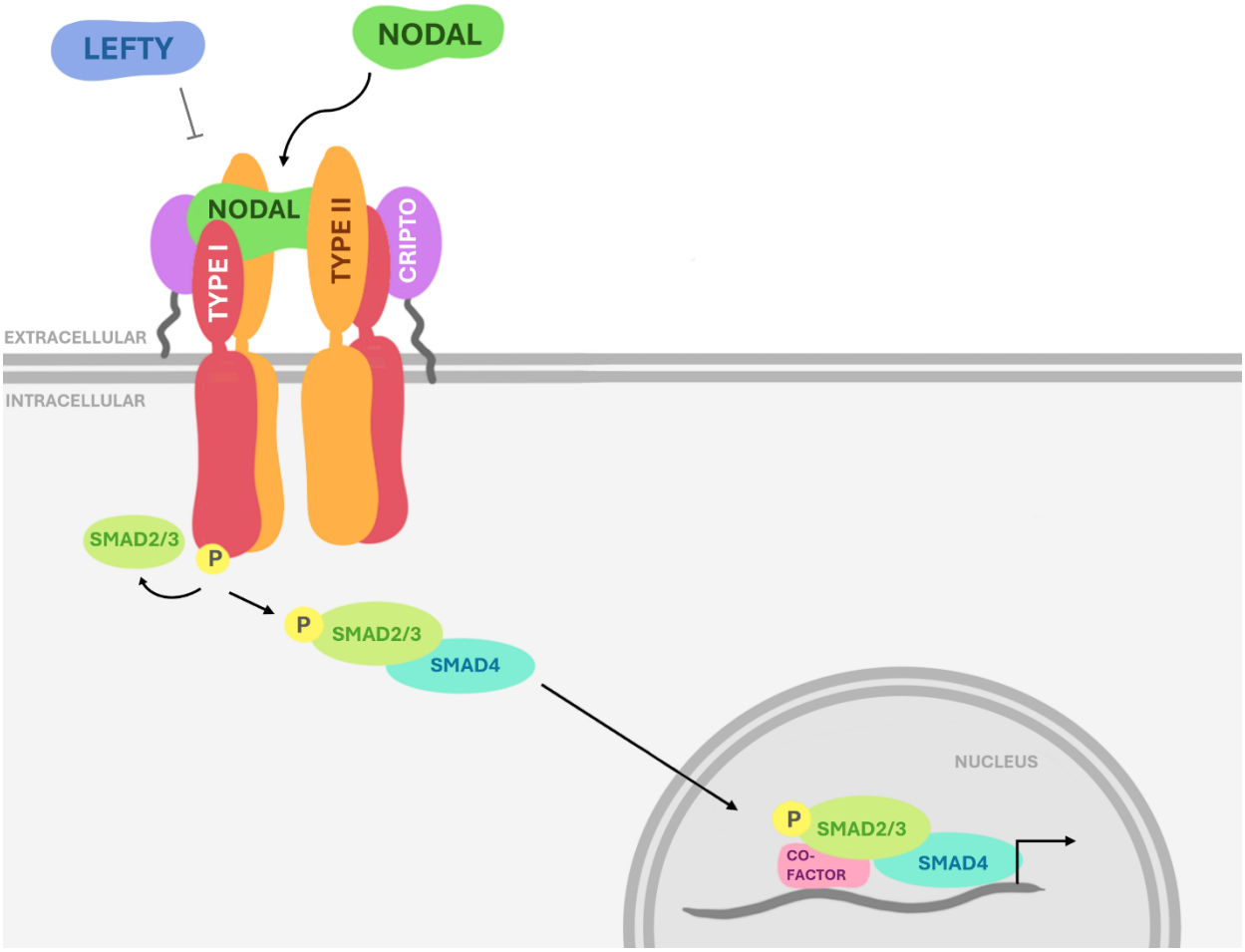

Figure 4: Canonical Nodal signaling pathway. Nodal ligands bind to type I (ALK4) and type II (ActRIIB) receptors on the cell membrane, alongside its co-receptor Cripto or Oep. This receptor complex phosphorylates intracellular Smad2 and Smad3 proteins, which then associate with Smad4 to form a complex that translocates into the nucleus. Once inside the nucleus, the Smad complex cooperates with transcriptional co-factors such as FOXH1 to activate target genes, including *goosecoid*, a key marker of the prechordal plate during embryonic development. Additionally, this signaling induces the transcription of inhibitors like Lefty, which regulate the pathway by providing negative feedback to modulate Nodal activity. Illustration created on Autodesk Sketchbook Pro.

1.5.3. Nodal in the vertebrate gonads

In comparison to other members of the TGF- β superfamily, Nodal's role in reproduction is not as widely understood. However, mouse studies have shown that Nodal regulates reproduction, such as placental development [58], and maintains inflammatory responses in the uterus during pregnancy [59]. Recently, Zayed et al., 2020 reported that Nodal inhibits follicle growth and induces oocyte maturation in the zebrafish ovary. Their research also demonstrated that *ndr1* and *ndr2* silencing decreases mRNA expression levels of key steroidogenic enzymes *cyp17a1* and *hsd3b2*, and membrane progestin receptor *paqr8* within stage IIIb ovarian follicles, the stage of follicles that can undergo hormone-induced maturation [60]. This suggests that Nodal may regulate steroidogenesis and oocyte maturation in the zebrafish ovary.

Like the ovary, Nodal's role in the testis, namely the adult testis, is also not as widely understood. In the fetal testis of mice and humans, Nodal is reportedly involved in the regulation of germ cell development and the establishment of the somatic niche [61,62]. It also regulates the expression of pluripotency factors, such as Oct4 and Sox2, and the proliferation and survival of germ cells [63]. This regulation is crucial for the formation of seminiferous cords, steroidogenesis, and the function of Sertoli cells, which are essential for supporting the germ cell population during fetal development [62,64]. Disruption of Nodal signaling can lead to impaired seminiferous cord formation, reduced androgen secretion, and decreased numbers of gonocytes — the precursors to sperm cells. These disruptions can later contribute to the development of testicular dysgenesis syndrome and testicular germ cell cancer in humans [65,66]. While its function in the zebrafish testis, and in general the adult testis, remains unknown, preliminary data from our lab suggests that the protein may be involved in testis development and spermatogenesis.

1.6. RATIONALE, OBJECTIVES & HYPOTHESES

Nodal signaling has been extensively studied during embryonic development, but its roles in adult gonads remain poorly understood. Our lab has previously shown that Nodal can regulate ovarian function, and several studies in mammals suggest that Nodal is also expressed in testicular germ cells. Since the number and state of germ cells can influence sexual differentiation and testis function, it is plausible that Nodal signaling similarly affects adult testis biology in zebrafish.

The primary objective of this study was to investigate the role of Nodal, specifically *ndr1*, and its role in adult zebrafish testis. To do this, testis explants were incubated *ex vivo* with recombinant human Nodal, followed by RNA sequencing to identify changes in gene expression, pathways enrichment, and alternative splicing, with a focus on Nodal pathway components and genes related to spermatogenesis. Additionally, we examined the sex ratios of offspring from mutant (*ndr1*$^{+/-}$) x WT crosses to explore potential effects of Nodal signaling on sexual differentiation.

We hypothesized that Nodal may influence adult zebrafish testis function by modulating gene networks involved in germ cell maintenance, spermatogenesis, and reproductive processes. Given its known roles in embryogenesis and ovarian regulation, we further expected that Nodal signaling could affect gonadal differentiation, potentially altering germ cell dynamics and feedback regulation of key pathway components, such as *ndr1* and *lefty* genes.

CHAPTER 2

METHODS

2.1. Animals

Zebrafish were kept in 3L acrylic tanks under a 14-h light, 10-h dark cycle within a high-density rack system specifically designed for zebrafish (Aquaneering Inc., San Diego, USA). The system was maintained at 28°C, pH 7.2. All fish were fed twice a day, once with commercial pellets (Zeigler Bros Inc.) and another with brine shrimp. York University's Animal Care Committee approved the use of zebrafish in this project and all experiments were conducted in compliance with the Guide to Case and Use of Experimental Animals published by the Canadian Council on Animal Care.

2.2. Mutant *ndr1* zebrafish

For sex ratio analyses, fish from a mutant *ndr1* line were genotyped using the heteroduplex mobility assay. This line of fish was generated and characterized by a previous student in our lab using CRISPR-Cas9 genome editing, which introduced a 7 bp deletion and subsequent frameshift mutation in the pro-peptide region of the *ndr1* gene. The 7 bp deletion was also confirmed via Sanger sequencing.

As previously characterized, homozygous *(ndr1*$^{-/-}$) mutants exhibited a lethal phenotype; heterozygous (*ndr1*$^{+/-}$) fish remained viable and were used alongside wild-type (WT) siblings as controls, where applicable.

2.3. Heteroduplex mobility assay for genotyping

Fish were anesthetized with tricaine methanesulfonate (MS-222; 50 mg/L, pH 7.0), and caudal fin clips were collected for DNA extraction. Genomic DNA was prepared using an alkaline lysis method, in which fin tissue was incubated in 50 mM NaOH at 95°C to lyse cells and release DNA,

followed by rapid cooling and neutralization with Tris-HCl (pH 8.0). Samples were briefly centrifuged to pellet tissue debris, and the supernatant containing genomic DNA was used directly for PCR amplification.

PCR amplification of the *ndr1* target region was performed using a T100 Thermal Cycler (Bio-Rad Laboratories) and gene-specific primers (forward: 5'-TGCGTGTGGATTATTACCTTGA-3'; reverse: 5'-ATGGCTGAAATGTTTTTCGTCT-3'; Sigma-Aldrich). The PCR program consisted of an initial denaturation step at 95 °C to separate DNA strands, followed by 38 cycles of denaturation (95°C), annealing (61°C), and extension (72°C) to amplify the target fragment. A final extension step ensured complete synthesis of all amplicons before samples were cooled to 4°C. PCR products were analyzed on 11% polyacrylamide gels prepared in 1× TBE buffer and electrophoresed for approximately 1 h at 150 V using a standard SDS-PAGE apparatus. Gels were stained with ethidium bromide and visualized using the AlphaImager™ Gel Imaging System (Alpha Innotech). Distinct banding patterns were used to determine genotypes: heteroduplex bands indicated $ndr1^{+/-}$ fish, while single homoduplex bands of 249 bp corresponded to $ndr1^{+/+}$ wild-type individuals.

2.4. Sex ratio analyses

To assess the impact of Nodal on sex determination of zebrafish during development, two types of breeding crosses were conducted. Due to the lethal phenotype of a complete knockout of *ndr1* in embryos, which prevented their progression to adulthood, heterozygous mutant adults were used for breeding. In the first cross, $ndr1^{+/-}$ males were paired with wild-type (WT) females. In the second cross, WT males were paired with $ndr1^{+/-}$ females. Within each cross, offspring from two parental crosses were raised under standardized conditions in a recirculating aquatic system

maintained at a constant temperature and pH. A regular feeding schedule, consisting of commercial pellets and brine shrimp, was provided throughout the fish's development.

In the first breeding cross (*ndr1*$^{+/-}$ male × WT female), offspring were genotyped via fin-clipping after four months post-fertilization (mpf), and in the second breeding cross (WT male × *ndr1*$^{+/-}$ female), offspring were genotyped after 7 mpf. A total of 240 offspring from each cross were genotyped, with 120 offspring each being from a different parental pair. The number of males and females for each genotype was recorded based on external morphology and confirmed by gonadal dissection when necessary. Sex ratios were determined for each genotype group, and the male-to-female ratios of *ndr1*$^{+/-}$ and WT offspring were compared between the two breeding pairs from each cross.

2.5. Age-dependent expression of ndr genes in zebrafish testis

To profile the expression of *ndr1*, *ndr2*, and *ndr3* in the testis at different stages of fertility, WT male zebrafish were euthanized with MS-222 (250 mg/L). Testis were collected from fish at three age groups: 4, 9, and 18 mpf. This range was selected based on the known sexual maturity at 3 months and the decline in fertility after 18 months. For each age group, five testis were collected and processed for RT-qPCR analyses.

2.6. *Ex vivo* testis culture

Testis were collected from 9-month-old WT male zebrafish and cultured in basal culture medium at 25°C, as outlined in the protocol established by Leal et al. (2009). While the culture system has been reported to sustain organs for up to 7 days, tissues were cultured for up to 24 hours in this study. To determine the time course effects of Nodal on testis function, one testis from each pair

was treated with 250 ng/mL rhNodal (R&D Systems, Minneapolis, MN), while the other served as a control. Testis were cultured for 6, 18, and 24 hours to assess time-dependent changes in gene expression. For dose-response analysis, testis were cultured for 24 hours with different concentrations of rhNodal (50, 100, and 250 ng/mL). Following incubation, testis were collected and processed for RT-qPCR to measure the expression of nodal signaling and steroidogenic marker genes.

2.7. RNA extraction and Real-Time PCR

Tissues were first homogenized using a mechanical homogenizer to break down the tissues into smaller fragments. The tissue samples were subjected to two 15-second bursts of sonication to ensure thorough yet gentle disruption of cell membranes; this was an especially useful step for fatty tissues such as the testis. Following sonication, samples were incubated on a thermoshaker at 4°C for 15 minutes at 600 rpm to further facilitate the release of cytoplasmic contents. After this, RNA was extracted using RNAzol® RT (Sigma-Aldrich, Burlington, MA) and cDNA was synthesized from 1 µg of RNA using M-MuLV reverse transcriptase (New England Biolabs, Ipswich, MA) as per manufacturer's instructions.

Gene expression was quantified using a QuantStudio™ Pro 6 Real-Time PCR System (Applied Biosystems). The qPCR reactions were performed in 10 µL reaction volumes containing 5 µL of 2X SYBR Green PCR Master Mix, 2 µL nuclease-free water, 2 µL of cDNA template (diluted 1:4 for target genes and 1:40 for housekeeping control), and 0.5 µL of forward and reverse primers (see Table 1 for a full list of primers). PCR cycling conditions were as follows: an initial denaturation step at 95°C for 10 minutes, followed by 40 cycles of 95°C for 15 seconds and 60°C for 1 minute.

Relative gene expression was determined using the ΔΔCt method and statistical analysis was performed in GraphPad Prism.

Table 1: List of primers used in RT-qPCR.

NCBI Gene ID	Gene	Orientation	Sequence
30516	***ef1α***	Forward	AGGACATCCGTCGTGGTAA
		Reverse	AGCCTTGGGGTTGTCTTCA
317743	***gapdh***	Forward	TCCGTCTTGAGAAACCTGCCA
		Reverse	TGGATGAACGGCAATCCCCA
799352	***ndr1***	Forward	CACAAGAGCGTTCATCATCCT
		Reverse	TGGGAAACACCAGGAATCAT
30292	***ndr2***	Forward	GGTCGGGAGATTCATAGCAG
		Reverse	CGTCCTCGCTTGACTTCTTT
338101	***ndr3***	Forward	GAAGGGGAATGTCCGAGTCC
		Reverse	ACGATCATGTCCTCGTGGTG
30145	***lft1***	Forward	AGGAGCCGAATGGAGATGCC
		Reverse	TCACAGTCTCCACTAGACCCAA
30146	***lft2***	Forward	CACAGGCCGATAAACCACGC
		Reverse	CGTGAATGGGAACCAGTCGTG
368254	***paqr8***	Forward	CATCTTGTCTGGTTATCGTCC
		Reverse	GCCACACTGAAACTGAGGTAG
373131	***hsd3b2***	Forward	GAGAAAAGCTGGTCCGACTGT
		Reverse	CTACCTCAATGCTGCTGGTGTA
399692	***cyp17a1***	Forward	ACAGGGGGAATCTACCTTATC
		Reverse	CCGAGACAAACACGCACC

2.8. RNA-sequencing sample preparation

Testis were collected from 9-month-old WT males and cultured *ex vivo* as described previously. Explants were treated with 250 ng/mL rhNodal and maintained with their respective controls for 18 hours. Extracted total RNA was purified using the Monarch® Spin RNA Cleanup Kit (50 µg) by New England Biolabs. According to sample submission guidelines provided by The Centre for Applied Genomics (TCAG), samples with a 260/230 ratio >2.0 were sent for quality check. Each

sample contained 400 ng of total RNA. The best 8 samples (4 control, 4 treatment) were selected for next-generation sequencing.

2.9. RNA-sequencing data processing and analyses

All RNA-seq library preparation, data processing and primary analyses were performed by TCAG. The facility carried out alignment to the reference genome and differential gene expression analysis using STAR, HTSeq, and DESeq2/edgeR according to their standard pipeline. In brief libraries were prepared using a stranded, paired-end RNA-seq protocol following the facility's standard procedures and sequenced to a target depth of approximately 30 million paired-end reads per sample. Raw reads were quality-checked with FastQC, adapters were trimmed using Trim Galore, and the trimmed reads were aligned to the Danio rerio reference genome (GRCz11, Ensembl release 113) using STAR v2.6.0c. Gene-level counts were generated with HTSeq-count, and differential expression was analyzed using DESeq2 v1.26.0 and edgeR v3.28.1 in R v3.6.1.

Normalization, filtering, and multiple testing correction (Benjamini–Hochberg FDR) were performed following standard DESeq2 and edgeR workflows. Initial principal component analysis (PCA) plots showed poor clustering of samples, indicating the presence of unwanted variation. To account for this, surrogate variable analysis (SVA) was used to identify two hidden sources of variation, which were included as covariates in the differential expression analyses. Including these surrogate variables improved sample clustering and was applied in all downstream analyses.

RNA-seq data from control and rhNodal-treated samples were analyzed separately by a biostatistics consultant to explore gene expression patterns, biological pathways, and differential

exon usage. Expression levels were normalized as FPKM (Fragments Per Kilobase per Million). To characterize the baseline transcriptional landscape of control testis, genes were ranked by FPKM and analyzed using g:Profiler [68] to identify Gene Ontology (GO) terms and pathways enriched among the most highly expressed genes. Pathway enrichment was performed using tools such as clusterProfiler [69] and limma-CAMERA [70] to find overrepresented GO terms and coordinated changes between groups. Differential exon usage was assessed with DEXSeq [71], and the potential functional impact of affected exons was predicted using InterProScan. More details on the methods and the main enriched pathways are provided in the Results, alongside the relevant figures and tables.

2.10. Statistical analysis

Real-time PCR data are presented as mean ± SEM. Sample numbers and statistical analyses tests conducted are indicated in figure legends. Unpaired t-test was performed for comparison between two groups. One-way ANOVA was performed for multiple group comparisons, followed by Tukey's multiple comparison test. Statistical significance was defined as $p < 0.05$. All statistical analyses were performed in GraphPad Prism. Data pertaining to DEGs, pathway level enrichment, and exon usage were considered statistically significant if the Benjamini–Hochberg–adjusted p-value (FDR) was < 0.05.

CHAPTER 3

RESULTS

3.1. Heterozygous knockout of *ndr1* has no effect on sex ratio

Sex ratio analyses were conducted to determine whether partial loss of *ndr1* function affects sexual differentiation, as Nodal signaling plays a key role in early developmental patterning and may indirectly influence gonadal development. To assess this, parental genotypes were first verified using a heteroduplex mobility assay (Fig. 5) to distinguish wild-type and heterozygous *ndr1* individuals. Heterozygous mutants were used since homozygous knockouts of *ndr1* exhibited a lethal phenotype during embryogenesis and could not develop into adulthood. This confirmed that the offspring analyzed for sex ratio originated from $ndr1^{+/-}$ × WT crosses. The offspring resulting from such crosses were raised and genotyped. Genotypic analysis of zebrafish offspring revealed no difference in male-to-female sex ratios among the progeny of $ndr1^{+/-}$ and WT crosses, regardless of the sex of the mutant parent (Fig. 6 & 7). In both experimental groups, offspring were genotyped after reaching sexual maturity — 4 mpf (Fig. 6) or 7 mpf (Fig. 7) — and showed little to no difference in the ratio of WT:mutant offspring. Sex ratios, though male-biased, did not differ across two independent breeding pairs per condition (Fig. 6B & D, Fig. 7B & D). Furthermore, within each clutch, the proportions of $ndr1^{+/-}$ and WT individuals also did not differ (Fig. 6A & C; Fig. 7A & C).

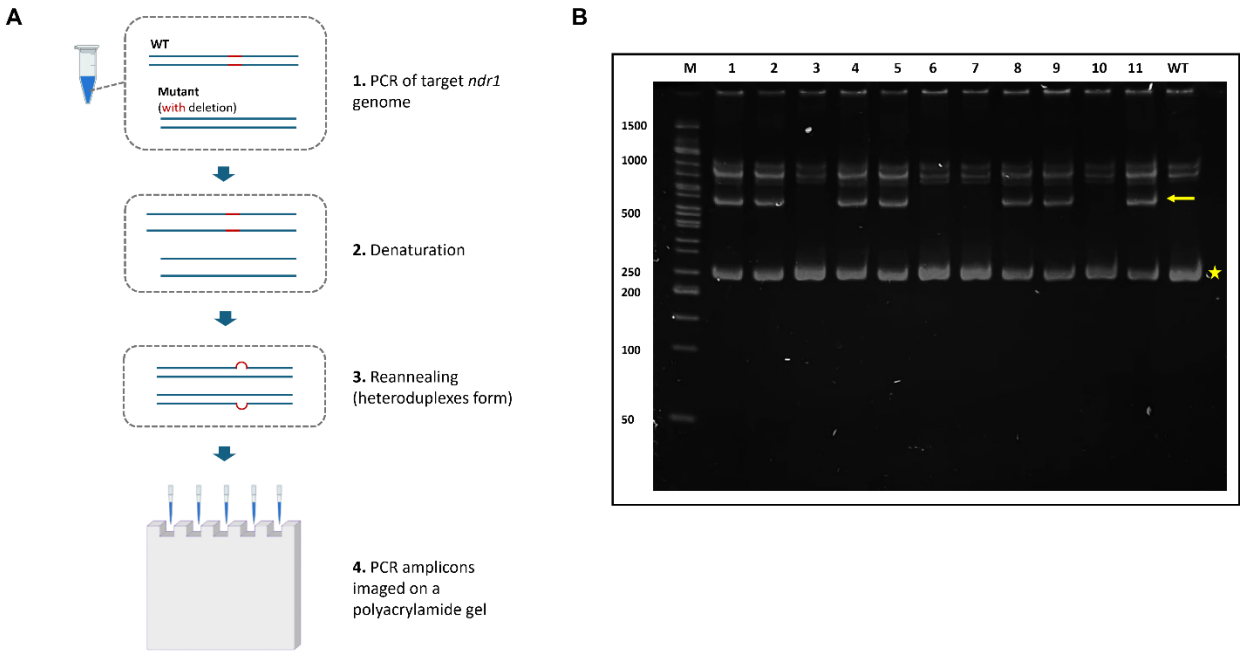

Figure 5: Schematic of heteroduplex mobility assay used to genotype *ndr1* zebrafish. (A) Summary of key steps in the heteroduplex mobility assay. Genomic DNA extracted from uncharacterized offspring of *ndr1* mutant × wild-type crosses was amplified and resolved on an 11% polyacrylamide gel. In heterozygous *ndr1* mutants, PCR amplification of both wild-type and mutant alleles followed by random re-annealing produced both matched homoduplexes and mismatched heteroduplexes, with the latter migrating more slowly on the gel due to structural distortions caused by the 7 bp deletion in the gene. (B) The expected wild-type homoduplex band (indicated by the star) was 249 bp, while the arrow denotes the heteroduplex, which migrated higher in the gel. Faint banding near 1 kbp observed across all samples likely represent PCR artifacts arising from abnormal duplex or multimer formation during heteroduplex re-annealing and were not considered in genotype determination. Lane M contains a 50 bp DNA ladder; lanes 1–11 show PCR amplicons from offspring of the *ndr1* line, and the final lane contains a known wild-type control amplicon. Figure created using assets from BioRender and Microsoft PowerPoint.

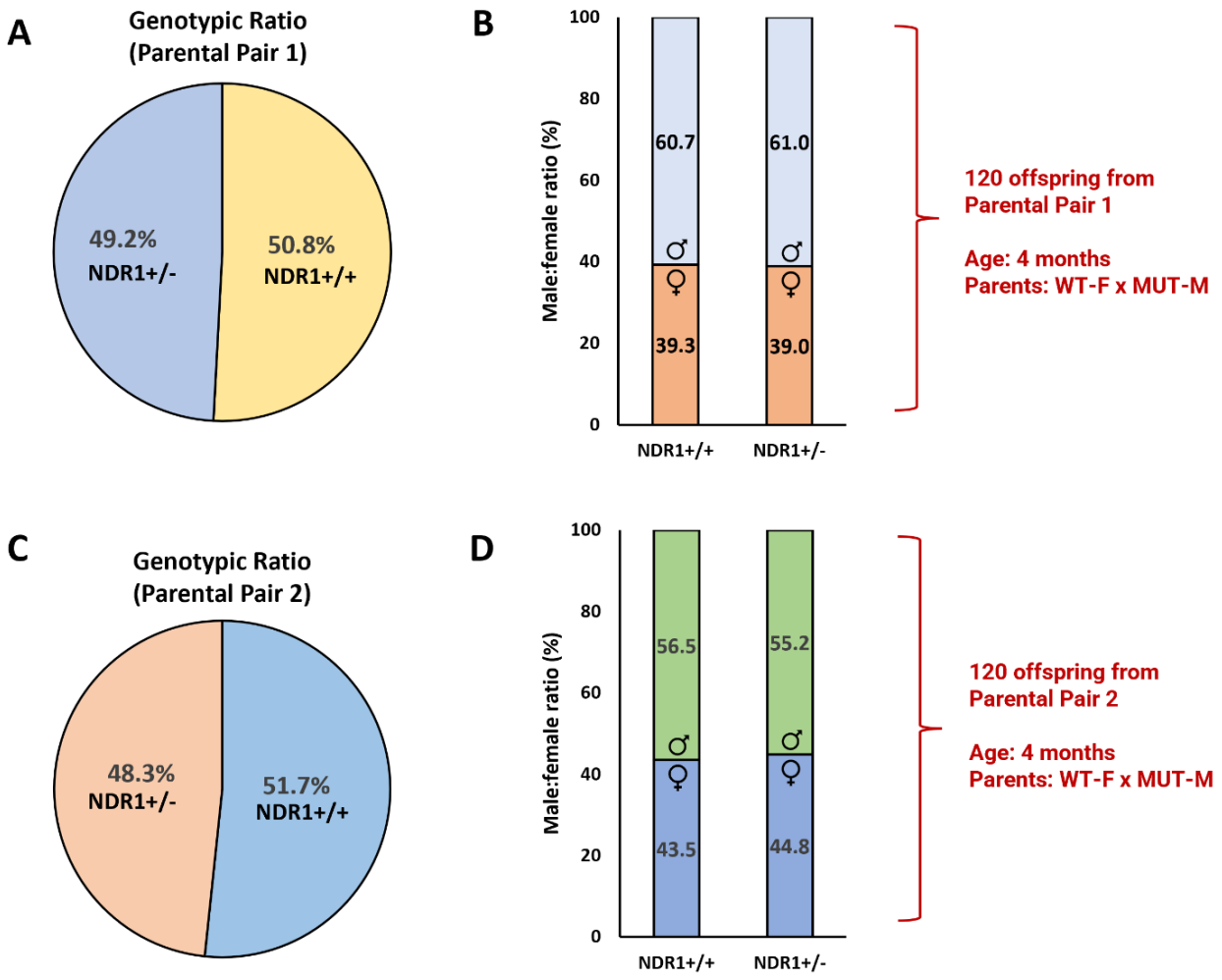

Figure 6: Male:female sex ratio zebrafish offspring of *ndr1*$^{+/-}$ male and WT female crosses. Zebrafish were raised until maturity on the same aquatic system under constant temperature and pH. A regular feeding schedule was also maintained for all fish. Four months post-fertilization, a total of 240 zebrafish were genotyped, 120 from one breeding pair (A) and another 120 which were the progeny of a different breeding pair (C). The number of WT (*ndr1*$^{+/+}$) and *ndr1*$^{+/-}$ males and females in each group of 120 fish was also noted (B, for the first group; D, for the second group).

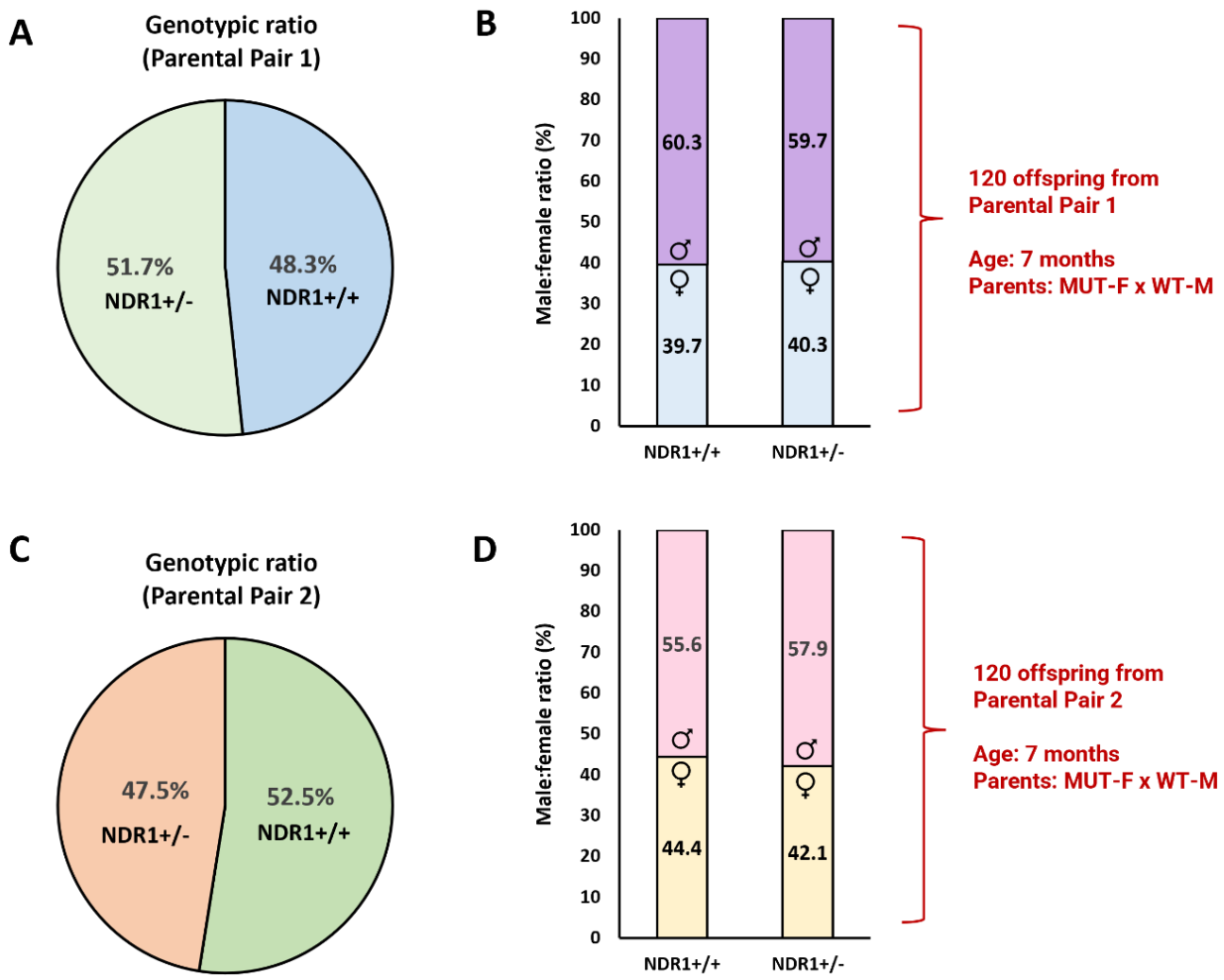

Figure 7: Male:female sex ratio in zebrafish offspring of WT male and *ndr1*$^{+/-}$ female crosses. Zebrafish were raised until maturity on the same aquatic system under constant temperature and pH. A regular feeding schedule was also maintained for all fish. Seven months post-fertilization, a total of 240 zebrafish were genotyped, 120 from one breeding pair (A) and another 120 which were the progeny of a different breeding pair (C). The number of WT (*ndr1*$^{+/+}$) and *ndr1*$^{+/-}$ males and females in each group of 120 fish was also noted (B, for the first group; D, for the second group).

3.2. Age-dependent expression of ndr genes in testis

Preliminary findings from our lab suggested that Nodal may play a role in zebrafish testis, particularly in adulthood. PCR data (unpublished) from other members in the lab indicated that *ndr1* was more highly expressed in the testis compared to *ndr2* and *ndr3*. To further investigate this, the potential involvement of Nodal in testicular function was examined.

Since zebrafish reach sexual maturity at 3 months and fertility begins to decline after 18 months, *ndr1*, *ndr2*, and *ndr3* expression was analyzed in WT testis at three different ages: 4, 9, and 18 months. Testis were collected from five males per age group and processed for RT-qPCR, with fold changes normalized to *gapdh*. As shown in Fig. 8, gene expression varied with age. Notably, *ndr1* was consistently expressed across all age groups but peaked in 9-month-old testis, while *ndr2* and *ndr3* levels were higher in older fish.

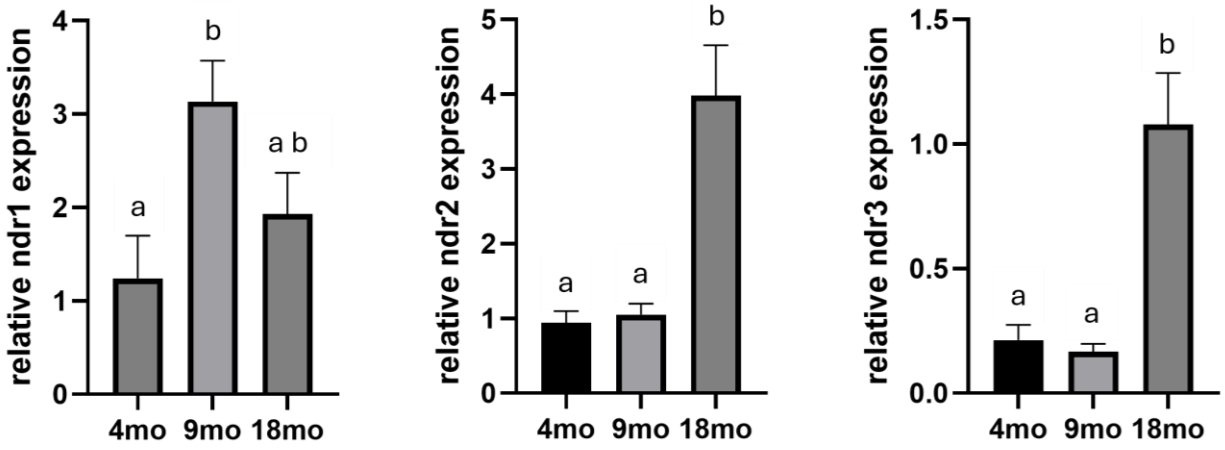

Figure 8: Age-dependent profiling of nodal-related genes in zebrafish testis. Expression levels of nodal-related genes (*ndr1, ndr2, ndr3*) were assessed across different age groups of zebrafish testis using RT-qPCR. Testis were collected from 4-, 9-, and 18-month-old WT males. Different letters above the bars indicate statistically significant differences between groups ($p < 0.05$, one-way ANOVA followed by Tukey's test). Bars sharing the same letter are not significantly different. Error bars represent ±SEM; n=5.

3.3. *Ex vivo* testis culture with recombinant human Nodal

Previous work from our lab demonstrated that treatment with rhNodal can activate phosphorylated Smad2 in zebrafish primary ovarian follicular cells [60]. Since phosphorylation of Smad2 is a marker of Nodal pathway activation, this suggests that rhNodal has biological activity in zebrafish. Based on this, an *ex vivo* testis culture experiment as outlined by Leal et al. (2009) was conducted to investigate if Nodal signaling could modulate gene expression in the zebrafish testis.

Testis were collected from 9-month-old WT males, when *ndr1* peaked in expression. Tissues were maintained in basal culture medium in 24-well plates with one testis being treated with rhNodal while the other remained as a control (Fig. 9). Incubation time and rhNodal concentration were based off those used in previously established ovarian follicular cell cultures that utilized rhNodal to stimulate *ndr1* and *ndr2* expression. For the time-course experiment, explants were treated with 250 ng/mL rhNodal for 6, 18, or 24 hours, while paired control testis were cultured without rhNodal. In the dose-response experiment, explants were treated with rhNodal at concentrations of 50, 100, and 250 ng/mL for 24 hours. Following culture, tissues were processed for RT-qPCR. Since Nodal is known to regulate its own expression through positive feedback and previous studies have shown that rhNodal treatment increases *ndr1/2* expression in ovarian follicles, *ndr1* expression was used as a positive control for rhNodal signaling in testis culture experiments. Nodal is also known to regulate the expression of its inhibitor Lefty via negative feedback; therefore, the expression of *lft1/2* was also quantified. Additional genes selected for analysis included *hsd3b2*, *cyp17a1*, and *paqr8* as previous studies in ovarian follicles demonstrated that *ndr1* silencing resulted in decreased expression of these genes.

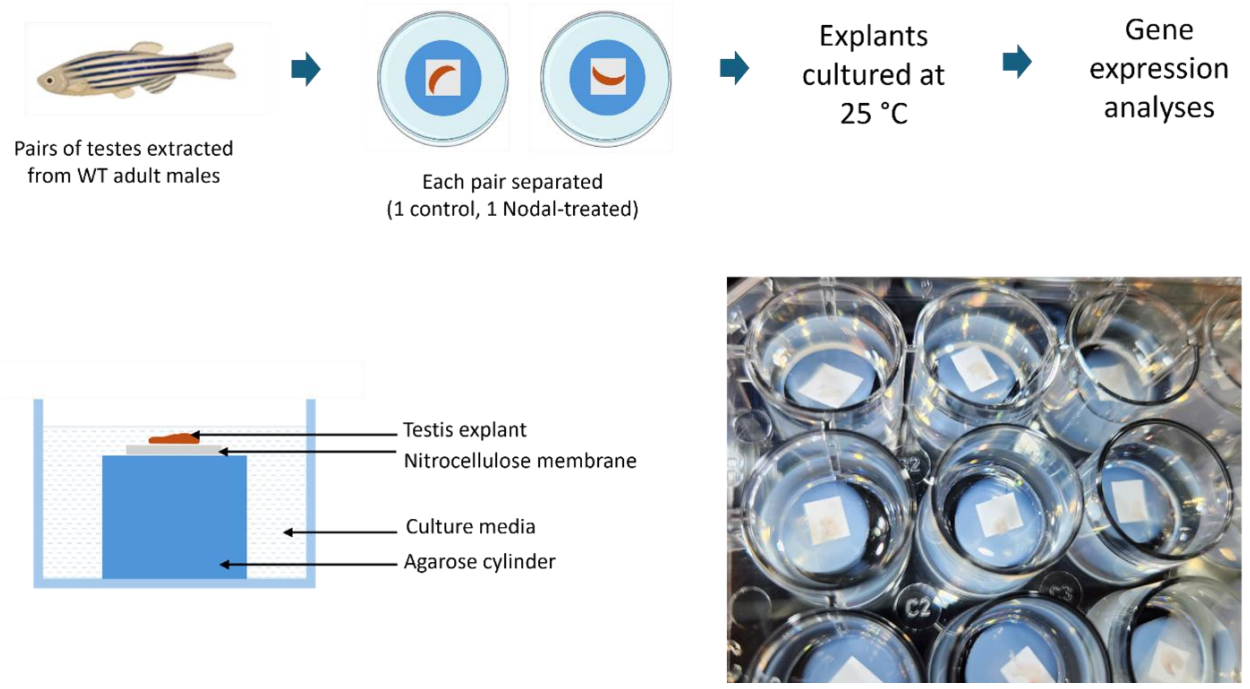

Figure 9: Schematic of *ex vivo* testis organ culture. Testis were extracted from 9-month-old WT males. One testis from each pair was treated with rhNodal (concentration dependent on the experiment) while the other served as a control. Testis were collected after incubation and processed for RT-qPCR. Figure created using assets from BioRender and Microsoft PowerPoint.

3.3.1. Time course expression analysis

Testis explants were cultured in 250 ng/mL rhNodal for 6, 18, and 24 hours and then collected for RT-qPCR analysis of Nodal signaling genes *ndr1* and *lft1/2.* Steroidogenic enzymes *hsd3b2, cyp17a1*, and membrane progestin receptor *paqr8* were also measured as our lab previously demonstrated that rhNodal induced the expression of these genes in ovarian follicles [60].

Fold changes were normalized to *ef1α* and are presented in Fig. 10 for Nodal signaling genes and Fig. 11 for steroidogenic and membrane receptor genes. Although the expression of *ndr1* appeared to have slightly increased in the treated testis after 18 and 24 hours of culture, these changes were not statistically significant. In contrast, *lft1*, a known inhibitor of Nodal signalling, exhibited a time-dependent increase. While *lft1* expression was not significantly altered at 6 or 18 hours, a significant upregulation was observed after 24 hours of rhNodal treatment ($p < 0.01$). Like *ndr1,* the other genes tested also did not demonstrate any significant changes in expression, though some slight variation in expression over the different time points could be observed.

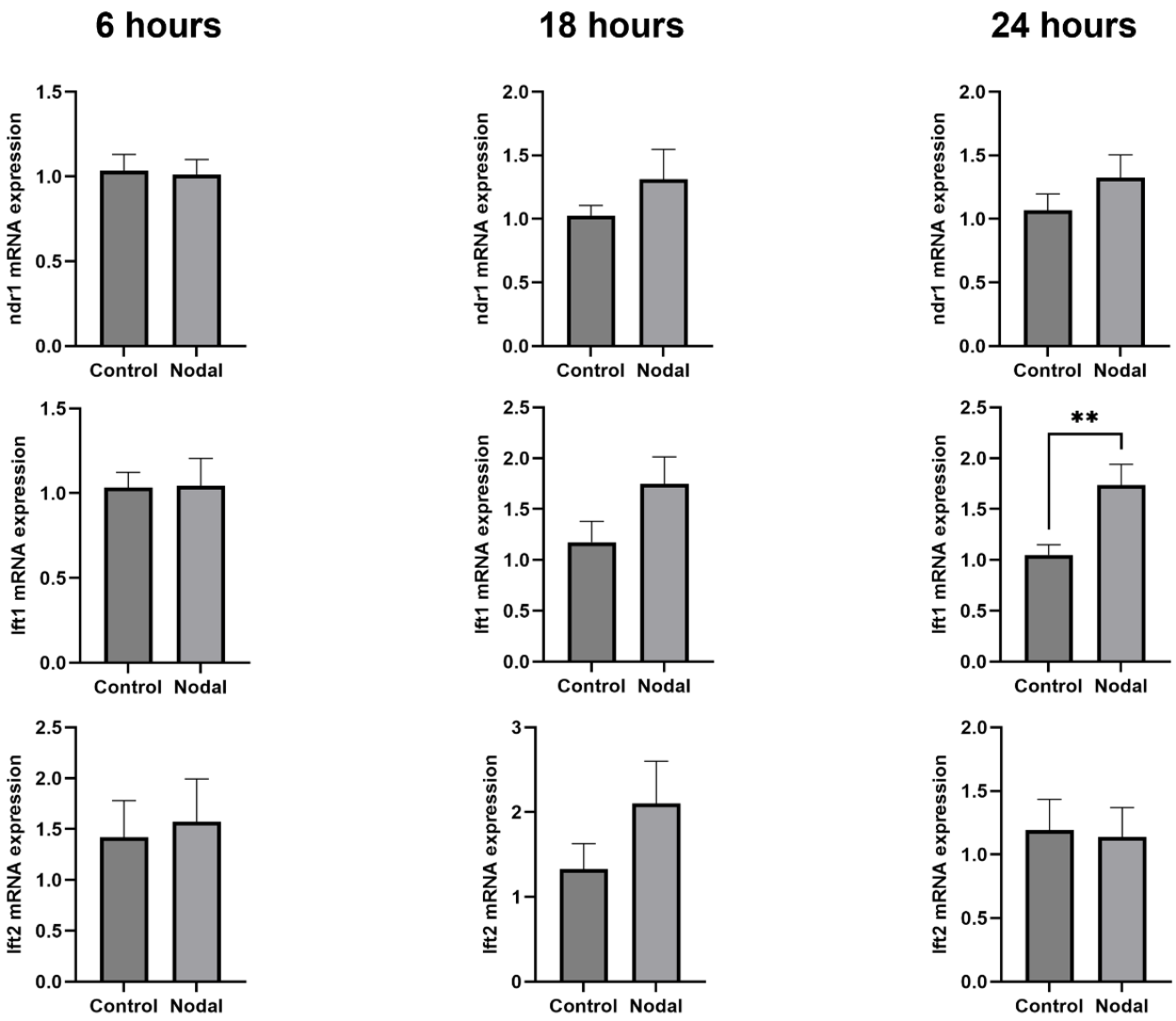

Figure 10: Relative expression of Nodal pathway genes in zebrafish testis cultured with rhNodal. Testis were cultured *ex vivo* for 6, 18, and 24 hours with 250 ng/mL rhNodal. Expression of *ndr1*, *lft1*, and *lft2* was quantified by RT-qPCR and normalized to *ef1α* expression. Statistical significance was determined using an unpaired t-test; **p <0.01. Data are presented as mean ± SEM (n = 10).

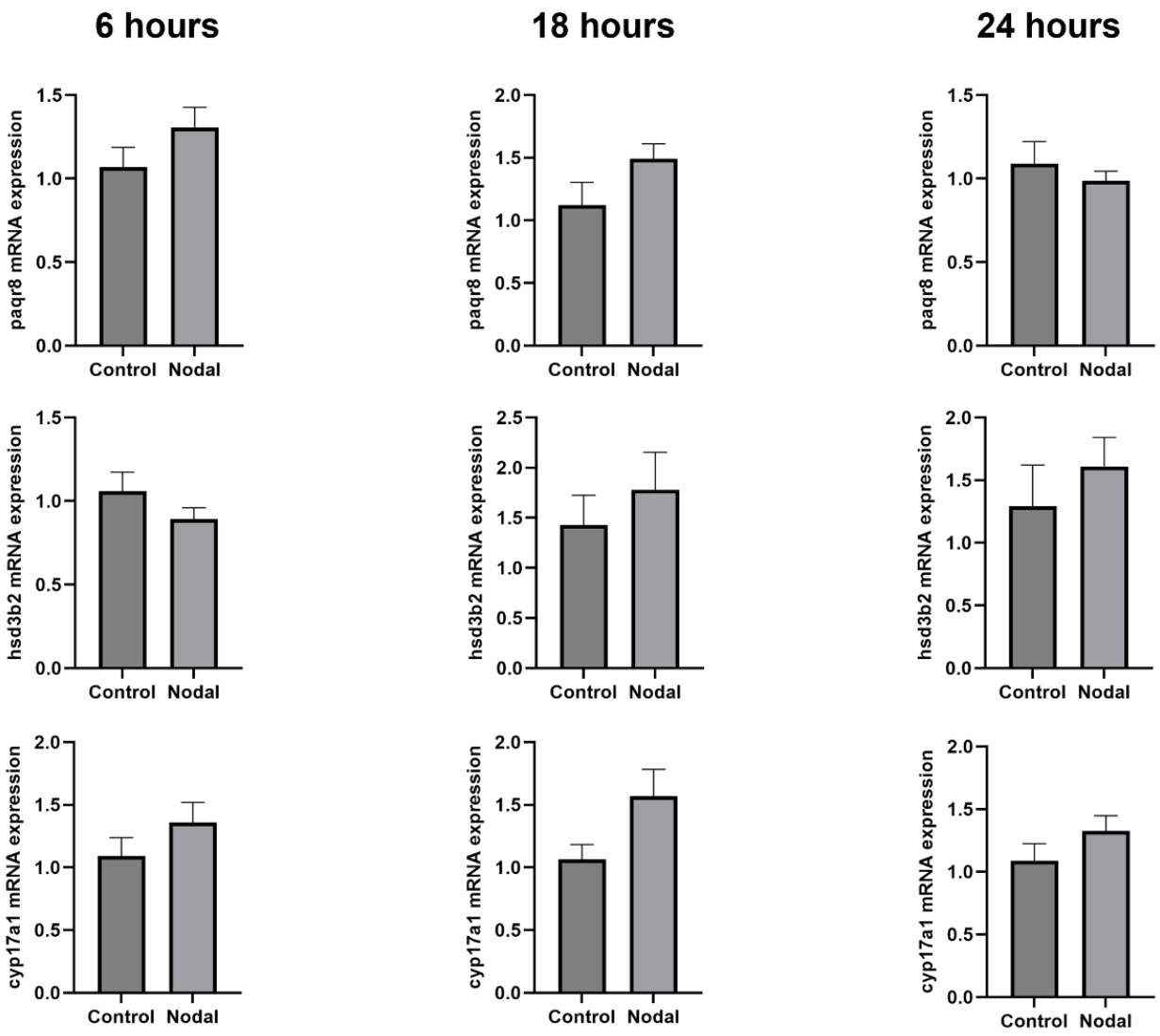

Figure 11: Relative expression of steroidogenic and membrane receptor genes in rhNodal-treated zebrafish testis. Testis were cultured in an *ex vivo* culture system for 6, 18, and 24 hours with 250ng/mL rhNodal. Gene expression was assessed using RT-qPCR. Steroidogenic enzyme genes (*cyp17a1, hsd3b2*), and membrane progestin receptor gene (*paqr8*) were analyzed. Fold changes normalized to *ef1α* housekeeping control. Statistical significance was determined using an unpaired t-test. Data are presented as mean ± SEM, n=10.

3.3.2. Dose-related response of rhNodal treatment

To evaluate dose-dependent effects of rhNodal treatment, testis explants from 9-month-old WT zebrafish were cultured for 24 hours with varying concentrations of rhNodal (0, 50, 100, 250 ng/mL), with the 0 ng/mL condition serving as the control. The expression of *ndr1* and *lft1* was analyzed by RT-qPCR. *Ndr1* was selected as the positive control for Nodal signaling, while *lft1* was chosen based on its response observed in the time-course experiment. As shown in Fig. 12, *ndr1* did not exhibit a clear dose-dependent trend, though its expression was highest at 250 ng/mL. In contrast, *lft1* displayed a more distinct dose-dependent response; however, statistical analyses also did not reveal any significant differences.

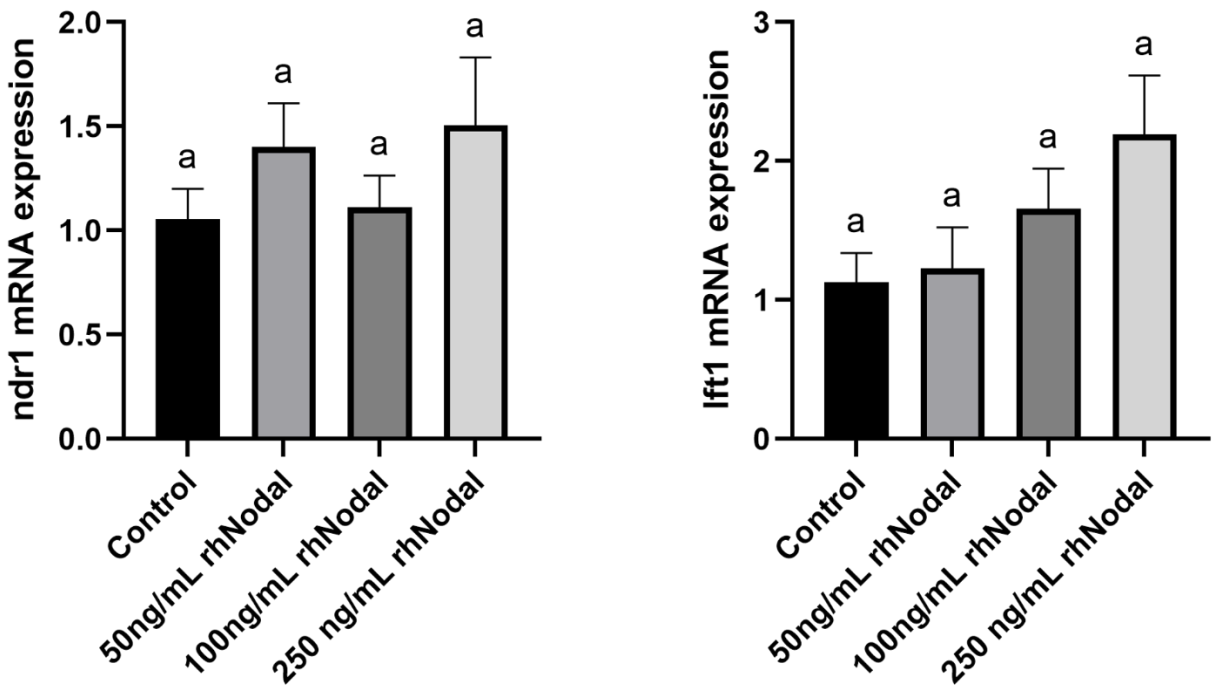

Figure 12: Dose-response expression of *ndr1* and *lft1* in zebrafish testis cultured with rhNodal. Testis were culture with 0 (control), 50, 100, and 250 ng/mL rhNodal for 24 hours. Gene expression was assessed using RT-qPCR. While *ndr1* expression remained unchanged, *lft1* expression was significantly increased at 250 ng/mL compared to the control. Fold changes normalized to *ef1α* mRNA levels. Statistical significance was determined using a one-way ANOVA followed by Tukey's test for multiple comparison. Bars sharing the same letter are not significantly different ($p>0.05$). Data are presented as mean ± SEM, n=6.

3.4. Differentially expressed genes in RNA-sequencing dataset

Using the *ex vivo* testis culture method, explants were incubated for 18 hours in 250 ng/mL rhNodal or left untreated. Total RNA was extracted and samples were sent to TCAG for next-generation sequencing and differential expression analysis. Quality checks showed that STAR alignment rates were >75% and over 60% of reads mapped to coding exons (see Appendix A, Fig. A1), reflecting generally good sequencing quality. As shown in Fig. A2, initial PCA and clustering plots showed poor separation of samples, indicating hidden variation. Including the two surrogate variables (SVs) identified by SVA improved clustering, suggesting that these sources of variation had been effectively accounted for. This approach allowed reliable identification of genes that changed expression between control and treated testis.

In total, 29,129 genes were detected across all samples. Differential expression analysis compared the Nodal-treated testis with the untreated controls to identify genes whose expression levels differed between the two conditions. As a result, 15,613 genes were identified as differentially expressed, of which only 24 genes were identified as significantly different. The volcano plot and heatmap illustrate this data (padj < 0.05; Fig. 13). A summary of significantly differentially expressed genes, excluding novel or unannotated transcripts, along with their human orthologs and known or predicted roles in testis, is provided in Table 2. Notably, some upregulated genes appeared to be associated with testis development and germ-cell function, including *klhl10b.2*, *atp1a1a.4*, and *h1m* while some downregulated genes are linked to innate immune function, including *pglyrp6*, *lyz*, and *cxcl12a*. None of the DEGs, however, correspond to canonical components of the Nodal signaling pathway.

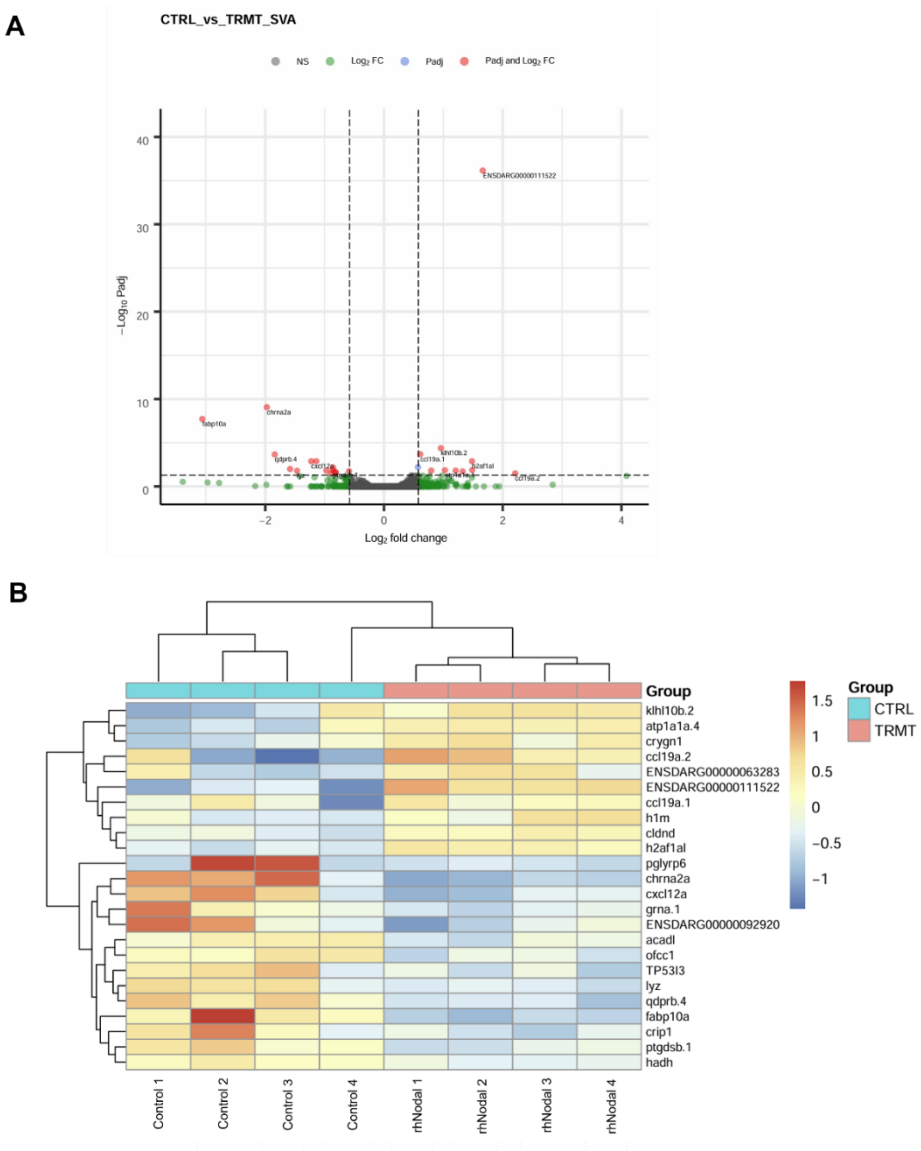

Figure 13: Differential gene expression in control vs. Nodal-treated zebrafish testis. Volcano plot (A) shows $\log_2$ fold change versus negative $\log_{10}$ adjusted p-value (-$\log_{10}$ padj) for each differentially expressed gene. Colours indicate significance and magnitude: grey = not significant, blue = padj < 0.05 only, green = |$\log_2$FC| above threshold only, red = both padj < 0.05 and |$\log_2$FC| above threshold. Log_2FC threshold was +/-0.585 and represents a 1.5x fold change. Positive $\log_2$FC indicates higher expression in treated samples, negative $\log_2$FC indicates higher expression in controls. Heatmap (B) shows genes up- or down-regulated between control and treatment groups. A total of 29,129 expressed genes were detected by RNA-seq, of which 15,613 were identified as differentially expressed. Of these, 24 genes were statistically significant based on adjusted p-value (padj < 0.05). Genes with higher expression in the treatment group are shown in red, and genes with higher expression in control are shown in blue.

Table 2: Summary of differentially expressed genes in zebrafish testis following rhNodal treatment. Listed are differentially expressed genes (excluding novel or unannotated transcripts) with their human orthologs, known or predicted functions in zebrafish, and any reported roles in testis. Information regarding gene function obtained from the Zebrafish Information Network database unless otherwise noted. Log_2 fold change (log_2FC) and adjusted p-values (padj < 0.05) are based on RNA-seq results; n=4.

Zebrafish Gene	Human Ortholog	Function in zebrafish	Role in testis?	log_2FC	padj
klhl10b.2	KLHL10	Ubiquitin ligase substrate adaptor [72]	Haploinsufficiency leads to male infertility (mice) [73]	0.959026	4.14E-05
atp1a1a.4	ATP1A1	Na^+/K^+-ATPase alpha subunit, ion transport	Ubiquitous; testis-specific isoform ATP1A4 involved in sperm capacitation [74] and motility [75]	1.026626	0.014095
crygn1	CRYGN	Crystallin, lens structural protein (predicted)	No reported testis function	0.7951	0.015309
ccl19a.2	CCL19	Predicted chemokine signaling	Immune function, expressed in all tissues; no reported testis function	2.210353	0.032219
ccl19a.1	CCL19	Predicted chemokine signaling	Immune function, expressed in all tissues; no reported testis function	0.610904	0.000205
h1m	H1.8	Chromatin linker histone	Expressed in primordial germ cells [76]	1.485679	0.013334
cldnd	CLDN4	Claudin family tight junction protein	Expressed in gonads; no direct testis function reported	1.20721	0.015401
h2af1al	H2A.J	H2A histone variant; embryonic mitotic cell cycle regulation	Expressed in ovary; no reported testis function	1.4818	0.001317
pglyrp6	PGLYRP2	Peptidoglycan recognition protein; immune defense against bacteria	No direct role in testis function	-1.58133	0.010119
chrna2a	CHRNA2	Nicotinic acetylcholine receptor α-subunit; neuronal receptor activity	No reported testis role	-1.97304	8.62E-10
cxcl12a	CXCL12	Chemokine; chemoattractant activity; cell migration/nervous system development	Not reported in zebrafish, but CXCL12/CXCR4 maintain postnatal spermatogonial population [77]	-1.22433	0.001317
grna.1	GRN	Granulin a; growth factor/inflammation/development roles in several tissue types	Neural roles; no specific testis roles reported	-0.81798	0.023126
acadl	ACADL	Fatty acid beta-oxidation enzyme; predicted mitochondrial matrix activity	Metabolic, not gonadal	-0.81102	0.02656
ofcc1	OFCC1	Developmental expression in eye/cranial neural crest	Craniofacial expression; no reported testis function	-1.14091	0.001317
tp53i3	TP53I3	p53-inducible gene involved in apoptosis, stress response	No reported direct role in testis	-0.96829	0.015309
lyz	LYZL1/2, etc.	Predicted to enable lysozyme activity; antibacterial enzyme	Reported roles of LYZL gene family in mammalian testis [78–80]	-1.46432	0.015887
qdprb.4	QDPR	Predicted quinoid dihydropteridine reductase activity	Metabolic, no gonadal data	-1.8403	0.000219
fabp10a	FABP1	Fatty-acid/bile-acid binding protein, lipid transport	Hepatic; no known testis role	-3.05874	1.95E-08
crip1	CRIP1	Cysteine-rich protein, predicted peptide and zinc binding activity	No reported testis function	-0.85722	0.006983
ptgdsb.1	PTGDS	Prostaglandin synthesis	Expressed in mammalian testis, may regulate sperm function [81]	-0.85949	0.014095
hadh	HADH	Hydroxyacyl-CoA dehydrogenase, fatty acid oxidation	No role reported in testis	-0.58763	0.017817

Looking specifically at the Nodal signaling pathway, several key genes were identified as differentially expressed between the control and treatment groups: the primary ligand *ndr1*, antagonists *lft1/2* and *dand5*, type I and II receptors (*acvr1ba/bb*, *acvr2aa/ba*), co-receptor *tdgf1*, intracellular mediators (*smad2*, *smad3a/b*, *smad4*), and downstream transcription factors (*mixl1* and *gata6*). However, while changes in expression of said genes were observed, none showed statistically significant differences in expression between treated and control testis. While *ndr2* was also detected in the overall dataset (i.e., present in the sequenced transcripts), it was not found to be differentially expressed. Meanwhile, *ndr3* was not detected at all in any sample. BaseMean values indicate that some Nodal pathway genes, such as *smad2* and *acvr2ba*, were among the more highly expressed transcripts overall (Table 3).

Table 3: Expression of key Nodal pathway genes in zebrafish testis RNA-seq dataset. Key Nodal signaling genes (*ndr1*, *lft1/2*, *dand5*, receptors, co-receptor, Smads, and downstream targets) are shown with their mean normalized read counts (BaseMean), $\log_2$ fold change, and adjusted p-value (padj). None showed statistically significant differential expression (padj < 0.05). NA in the padj column indicates genes filtered out by DESeq2 due to low counts.

Gene	Gene Name & Function	Role in Nodal Pathway	BaseMean	$\log_2$FC	padj
ndr1	Nodal-related 1 (Squint)	Primary Nodal ligand	251.8873411	0.070935525	0.999728877
lft1	Lefty1	Nodal inhibitor [82]	74.89703855	0.465684025	0.999728877
lft2	Lefty2	Nodal inhibitor [82]	127.2157456	-0.380837423	0.999728877
dand5	Cerberus/Dand5 (Antivin)	Nodal antagonist [83]	47.88501065	-0.222175607	NA
acvr1ba	Activin receptor type-1B, paralog a (ALK4)	Type I receptor	289.7112112	0.156567254	0.999728877
acvr1bb	Activin receptor type-1B, paralog b (ALK4)	Type I receptor	51.42096804	-0.076518396	NA
acvr2aa	Activin receptor type-2A, paralog a	Type II receptor	433.8796639	-0.307333161	0.999728877
acvr2ba	Activin receptor type-2B, paralog a	Type II receptor	485.4665923	-0.016284906	0.999728877
tdgf1	Cripto	Co-receptor for Nodal ligands [55]	154.8355305	0.167721672	0.999728877
smad2	SMAD2	Intracellular signal transducer	1028.349245	-0.006286872	0.999728877
smad3a	SMAD3a	Intracellular signal transducer	197.4404862	0.142779354	0.999728877
smad3b	SMAD3b	Intracellular signal transducer	156.9221081	-0.291640102	0.999728877
smad4	SMAD4	Mediator SMAD	160.1489164	0.235266423	0.999728877
mixl1	Mix-like 1	Transcriptional target of Nodal [84]	47.92597786	-0.001294364	NA
gata6	GATA6	Transcription factor, downstream target [85]	371.3119088	0.134943878	0.999728877

3.5. Pathway enrichment and differential exon usage analyses

3.5.1. Enriched pathways and genes in control testis

To understand which biological processes were most active under untreated conditions, an over-representation analysis was performed using clusterProfiler. Instead of focusing on differentially expressed genes, this analysis used the top 10% most highly expressed genes from the control group based on the raw sequencing counts provided by TCAG. This was done under the assumption that more highly expressed genes play critical roles in cellular function. This approach helped identify the main pathways that were active in the testis under baseline conditions, providing a reference for later comparison with the treated samples. The analysis looked at GO terms, which are standardized categories used to describe gene function. GO terms fall into three groups: Biological Process (the broader cellular or physiological role), Molecular Function (what the gene product does), and Cellular Component (where it acts in the cell). The results were clustered by semantic similarity, where terms with similar biological meanings were grouped together to avoid redundancy. For example, several terms describing different parts of RNA processing would be grouped into a single cluster.

The top 20 enriched terms were plotted by GeneRatio (the proportion of genes associated with each term), with color intensity representing statistical significance (adjusted p-value; Fig. 14). The most enriched processes were related to RNA processing and protein synthesis, including ribonucleoprotein complex biogenesis, RNA splicing, and cytoplasmic translation. Additional enriched pathways involved organelle organization (mitochondrion organization, chromosome

organization, microtubule cytoskeleton organization) and metabolic activity, such as oxidative phosphorylation, cellular respiration, and purine nucleotide biosynthesis.

To characterize the functional themes of genes most highly expressed in the control zebrafish testis, a ranked-based enrichment approach was used to avoid reliance on an arbitrary expression cutoff (e.g., the top 10%). Genes were ranked according to their average FPKM values across control replicates, and enrichment of annotation terms (GO, KEGG, Reactome, etc.) was assessed progressively from the top of the ranked list downward. The g:Profiler Ordered Query mode identifies terms whose associated genes are non-randomly concentrated near the top of the ranked list. Statistical significance in this context indicates that genes associated with a given pathway or functional category tend to occur among the most highly expressed transcripts more often than expected by chance, rather than representing classical overrepresentation. This approach complemented the clusterProfiler results, highlighting pathways such as cytosolic ribosomal subunits, mitochondrial ATP synthesis, and Notch signaling among the top-expressed genes, providing additional insight into the dominant functional themes in the baseline testis transcriptome (Table 4).

Together, these results highlight the major molecular processes active under baseline conditions in the control testis.

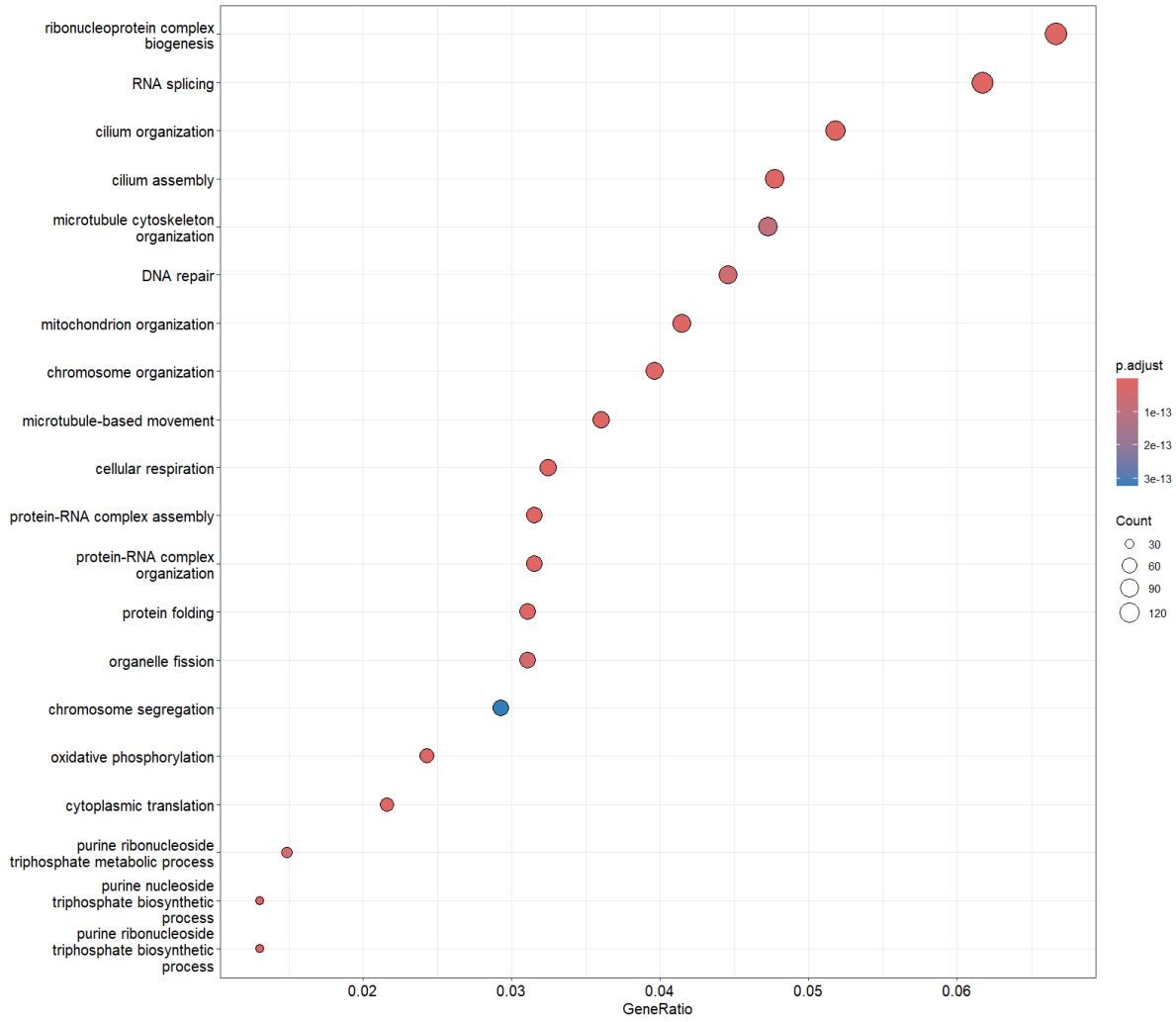

Figure 14: GO pathway enrichment of the top 10% most highly expressed genes in control samples. Over-representation analysis was performed using clusterProfiler, and related GO terms were clustered by semantic similarity. The x-axis shows the GeneRatio, or the proportion of input genes associated with each GO term, representing the strength of enrichment. Circle size corresponds to the number of genes associated with each term while colour represents statistical significance (adjusted p-value). Only the top 20 enriched GO terms are shown.

Table 4: Enriched GO terms among highly expressed genes in control zebrafish testis. Genes were ranked by expression level, and g:Profiler Ordered Query analysis identified GO categories non-randomly enriched near the top of the ranked list. Adjusted p-values (padj) indicate the significance of enrichment, with $-\log_{10}$ padj values shown for comparison. Leading genes represent those contributing most to each GO term's enrichment.

GO Term/Pathway	Source	padj	$-\log_{10}$ padj	Leading Genes
Cytosolic ribosome (GO:0022626)	GO:CC	2.21e-14	13.656051371356945	*rplp2l, rpl12, rpl23a, rps23, rpl14, rpl13a, rpl3, rpl29, rpl28, rpl37a, rps19*
Cytosolic large ribosomal subunit (GO:0022625)	GO:CC	4.54e-12	11.34297612702199	*rplp2l, rpl12, rpl23a, rpl14, rpl13a, rpl3, rpl29, rpl28, rpl37a*
Ribosomal subunit (GO:0044391)	GO:CC	5.05e-10	9.296918918459127	*rplp2l, rpl12, rpl23a, rps23, rpl14, rpl13a, rpl3, rpl29, rpl28, rpl37a, rps19*
Large ribosomal subunit (GO:0015934)	GO:CC	4.52e-9	8.345267305213756	*rplp2l, rpl12, rpl23a, rpl14, rpl13a, rpl3, rpl29, rpl28, rpl37a*
Cristae formation (REAC:R-DRE-8949613)	REAC	0.000368	3.4342136097962532	*mt-atp6, atp5l, atp5mc3b, atp5f1b,atp5po, atp5fa1, atp5mea, atp5pd, atp5mc1, atp5mc3a, atp5pf*
Formation of ATP by chemiosmotic coupling (REAC:R-DRE-163210)	REAC	0.000368	3.4342136097962532	*mt-atp6, atp5l, atp5mc3b, atp5f1b,atp5po, atp5fa1, atp5mea, atp5pd, atp5mc1, atp5mc3a, atp5pf*
Activated NOTCH1 transmits signal to the nucleus (REAC:R-DRE-2122948)	REAC	0.00994	2.0025508628573783	*uba52, rps27a*
ER Quality Control Compartment (REAC:R-DRE-901032)	REAC	0.00994	2.0025508628573783	*uba52, rps27a*
Signaling by NOTCH (REAC:R-DRE-157118)	REAC	0.00994	2.0025508628573783	*uba52, rps27a*
Signaling by NOTCH1 (REAC:R-DRE-1980143)	REAC	0.00994	2.0025508628573783	*uba52, rps27a*
Calnexin/calreticulin cycle (REAC:R-DRE-901042)	REAC	0.0198	1.7035467866088236	*uba52, rps27a*
E3 ubiquitin ligases ubiquitinate target proteins (REAC:R-DRE-8866654)	REAC	0.0198	1.7035467866088236	*uba52, rps27a*
RIPK1-mediated regulated necrosis (REAC:R-DRE-5213460)	REAC	0.03289	1.4837232973647452	*uba52, rps27a*
Regulation of necroptotic cell death (REAC:R-DRE-5675482)	REAC	0.03289	1.4837232973647452	*uba52, rps27a*
Granulocytic hypoplasia (HP:0012139)	HP	0.0449	1.3481391263296243	*rpl18, rpl26*

3.5.2. Comparative pathway enrichment (treatment vs. control)

A process similar to the commonly used gene set enrichment analysis (GSEA) was conducted to assess how Nodal exposure alters gene activity in zebrafish testis (Fig. 15). Because standard differential expression analysis did not identify major transcript-level differences between groups, a non-parametric competitive gene set test (using the tool, CAMERA) was used in combination with clusterProfiler to evaluate pathway-level changes. Unlike conventional parametric tests that assess individual gene expression values, this approach ranks all genes according to their relative expression differences and identifies pathways in which genes show consistent shifts in rank between conditions. This method is suitable for detecting subtle or coordinated transcriptional responses that may not be evident at the single-gene level.

The top enriched GO biological process terms were largely associated with protein synthesis and ribosomal activity, including ribosome, structural constituent of ribosome, translation, cytosolic large ribosomal subunit, and ribonucleoprotein complex (Fig. 15A). These pathways appeared to be downregulated in the Nodal-treated samples. Additional enriched categories were related to reproductive processes, such as binding of sperm to zona pellucida, acrosin binding, and egg coat organization. The genes reflected in these GO terms consisted of zona pellucida (ZP) family members, such as *zp3a1* and *zp3a2*, which were upregulated in the Nodal-treated testis. Enrichment of pathways involved in mitotic cell cycle regulation (upregulated) and formation of cytoplasmic translation initiation complexes (downregulated) was also observed. A comprehensive list of the direction of regulation and representative genes within each GO biological process term can be found in Table 5.

The complementary enrichment analysis visualized in the clusterProfiler dot plot (Fig. 15B) similarly highlighted pathways related to RNA and protein complex assembly (protein–RNA complex assembly, ribonucleoprotein complex biogenesis) and peptide biosynthesis. Notably, several immune-related pathways were also enriched, including immune response, defense response to bacterium, and immune effector process. All of these processes, except for protein autophosphorylation (which was upregulated), were downregulated in the treatment samples (Table 6).

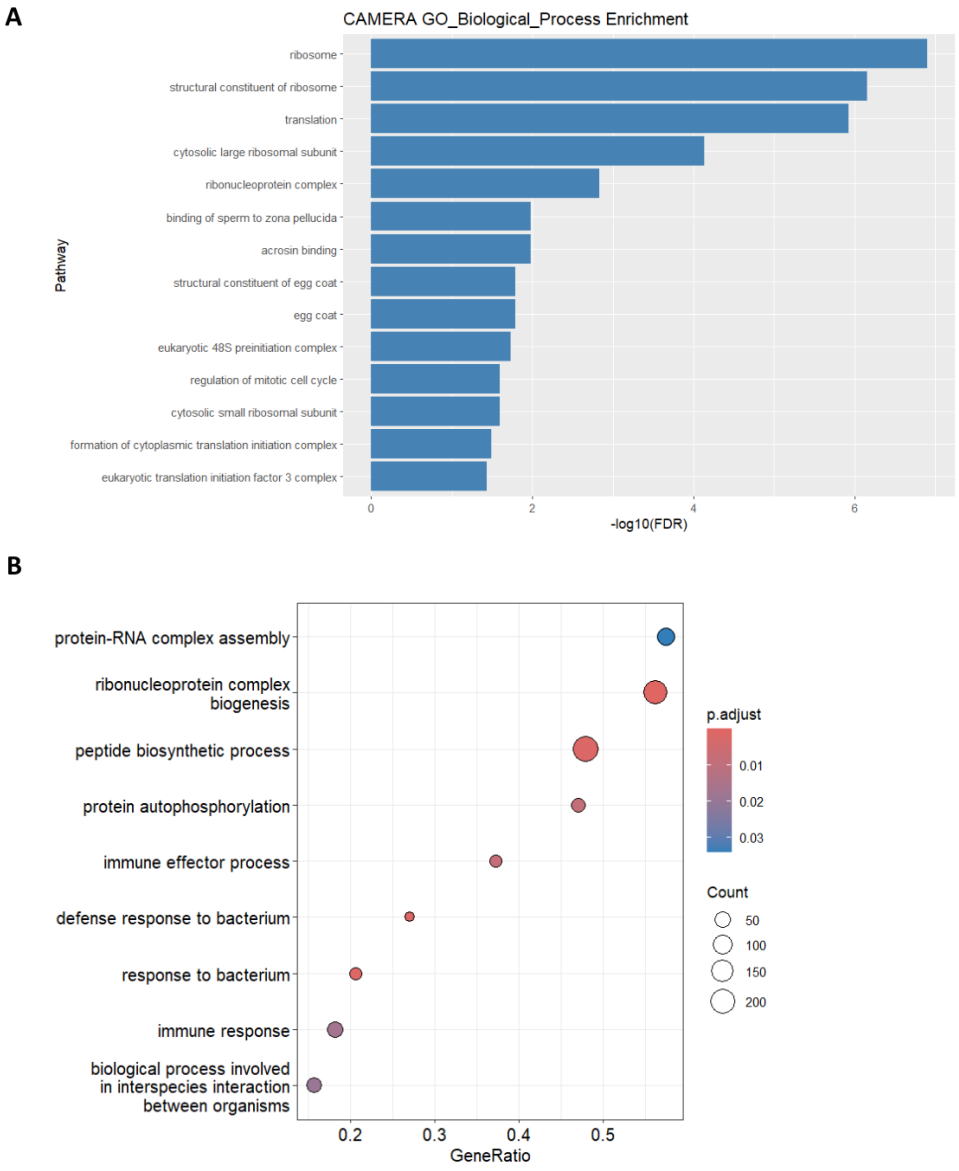

Figure 15: GO pathway enrichment in Nodal-treated and control samples. (A) CAMERA analysis (competitive gene set test from the R package limma) was applied to $\log_2$-transformed FPKM values to identify GO Biological Process pathways showing coordinated up- or down-regulation in the treatment group, regardless of whether individual genes showed significant expression change. Only terms with FDR < 0.05 are plotted. (B) clusterProfiler analysis was conducted on genes ranked by $\log_2$ fold change ($\log_2$FC = treatment - control) using a GSEA-like approach and permutation testing was used to identify pathways whose member genes were collectively up- or down-regulated. Circle size represents the number of genes associated with each GO term, and GeneRatio indicates the proportion of input genes mapped to that term.

Table 5: GO terms identified by CAMERA analysis with associated genes and direction of regulation. This table supplements Figure 15A by showing the specific genes contributing to each enriched GO term and whether the pathway was up- or downregulated in Nodal-treated testis. Analysis was performed on log_2-transformed FPKM values using CAMERA from the limma R package, focusing on GO Biological Process terms with FDR < 0.05. The direction column indicates the overall trend for the pathway, while the Genes column lists some of the representative members driving the enrichment signal.

GO_ID	GO Biological Progess	Number of Genes	Direction	PValue	FDR	Genes
GO:0005840	ribosome	135	Down	1.44e-11	1.24e-07	*mrpl51, rpl5a, rps28, rps27.1*
GO:0003735	structural constituent of ribosome	124	Down	1.61e-10	6.94e-07	*mrpl51, rpl5a, rps28, rps27.1*
GO:0006412	translation	179	Down	4.12e-10	1.19e-06	*mrpl51, rpl5a, rps28, rps27.1*
GO:0022625	cytosolic large ribosomal subunit	44	Down	3.38e-08	7.30e-05	*rpl5a, rpl5b, rpl21, rpl36*
GO:1990904	ribonucleoprotein complex	218	Down	8.49e-07	0.00147	*mrpl51, rpl5a, rps28, rps27.1*
GO:0007339	binding of sperm to zona pellucida	11	Up	8.52e-06	0.0105	*zp3a.1, zp3a.2, zp3d.2, zp3c*
GO:0032190	acrosin binding	11	Up	8.52e-06	0.0105	*zp3a.1, zp3a.2, zp3d.2, zp3c*
GO:0035804	structural constituent of egg coat	8	Up	1.70e-05	0.0163	*zp3a.1, zp3a.2, zp2.3, zp2.6*
GO:0035805	egg coat	8	Up	1.70e-05	0.0163	*zp3a.1, zp3a.2, zp2.3, zp2.6*
GO:0033290	eukaryotic 48S preinitiation complex	13	Down	2.14e-05	0.0185	*eif3hb, eif3ea, eif3ha*
GO:0007346	regulation of mitotic cell cycle	47	Up	3.51e-05	0.0255	*pimr120, afap1l2, cdkn1a*
GO:0022627	cytosolic small ribosomal subunit	29	Down	3.54e-05	0.0255	*rps28, rps27.1, rps10, rps15*
GO:0001732	formation of cytoplasmic translation initiation complex	12	Down	4.83e-05	0.0321	*eif3hb, eif3ea, eif5, eif3ha*
GO:0005852	eukaryotic translation initiation factor 3 complex	11	Down	5.92e-05	0.0366	*eif3hb, eif3ea, eif5, eif3ha*

Table 6: Enriched GO terms identified by clusterProfiler analysis. Genes were ranked by log_2 fold change (treatment – control), and permutation testing identified GO biological processes whose member genes were collectively up- or down-regulated. The table lists significantly enriched biological processes (padj < 0.05), along with the number of genes in each set, normalized enrichment score (NES), p-value (pvalue), adjusted p-value (padj). Negative NES values indicate downregulation in Nodal-treated samples, whereas positive NES values indicate upregulation.

GO_ID	GO Term/Pathway	Number of Genes	NES	PValue	padj
GO:0022613	ribonucleoprotein complex biogenesis	315	-2.07387	1.83e-09	7.39e-06
GO:0042742	defense response to bacterium	48	-2.35371	8.32e-07	0.000841
GO:0009617	response to bacterium	97	-2.22298	5.48e-07	0.000841
GO:0042254	ribosome biogenesis	227	-2.01016	6.80e-07	0.000841
GO:0043043	peptide biosynthetic process	465	-1.75207	2.06e-06	0.001663
GO:0006412	translation	461	-1.75465	2.84e-06	0.001918
GO:0002252	immune effector process	51	-2.2211	1.40e-05	0.008067
GO:0046777	protein autophosphorylation	66	2.093871	1.74e-05	0.008804
GO:0006955	immune response	247	-1.77253	3.81e-05	0.017118
GO:0044419	biological process involved in interspecies interaction between organisms	247	-1.75018	4.78e-05	0.019331
GO:0022618	protein-RNA complex assembly	122	-1.93306	9.29e-05	0.034167

3.5.3. Differential exon usage

To complement the gene-level expression analyses conducted by TCAG, differential exon usage was assessed to identify specific exons and detect transcript-level changes that might not appear in overall gene expression. This analysis evaluated changes in expression at the exon level, rather than the whole gene, providing insight into potential alternative splicing events. Examining exon-level variation helps identify alternative splicing events that could influence protein function or signaling activity in the testis.

Log_2 fold changes were calculated for each exon, and adjusted p-values were used to determine significance. Significant exons indicate those that are more or less utilized in one group relative to the other, although the analysis does not allow full reconstruction of the transcript isoform to which the exon belongs.

Several exons showed significant differential usage between the treatment and control groups (Table 7). These included: *insra* (ortholog of human INSR), *klhl10b.1* (ortholog of KLHL10), and *chrna2a*, which had two exons differentially used; the upregulated exon in the treatment group is predicted to encode a neurotransmitter-gated ion-channel transmembrane region, while the downregulated exon may encode a nicotinic receptor ligand-binding domain relevant to spermatogenesis.

Table 7: Differential exon usage and function prediction between control and treatment. Exon-level expression was quantified using FeatureCounts, and differential usage was assessed with DEXSeq. The table lists genes with significant differential exon usage (padj < 0.05), along with predicted functional domains of the affected exons as determined by InterProScan. Positive log_2 fold change values indicate more usage of exon in the treatment group, while negative values indicate less exon usage. Note: klhl10b.1_1 is an alternative locus to klhl10b.1 (on chr NC_007128.7).

Gene	NCBI_chr	chr_start	chr_end	strand	Protein domain prediction	padj	log_2fold
insra	NC_007113.7	37631822	37632908	-	5'UTR + Signal peptide (N-, H-, and C-regions) + non-cytoplasmic domain	0.01071	0.93717
rtkna	NC_007116.7	43612031	43617869	-	Intrinsically disordered regions (IDR) + 3'UTR	0.03406	0.26256
chrna2a	NC_007128.7	6096747	6097800	+	Nicotinic receptor ligand binding domain-like + Neurotransmitter-gated ion-channel transmembrane	0.00582	-0.52453
chrna2a	NC_007128.7	6100975	6101820	+	Neurotransmitter-gated ion-channel transmembrane + 3'UTR	0.04989	0.82970
LOC137489247	NC_007135.7	25363514	25363570	+	unannotated lncRNA	0.04989	-2.52047
klhl10b.1_1	NW_018394976.1	198951	199067	+	Kelch motif	0.04989	1.23434
klhl10b.1_1	NW_018394976.1	199459	199550	+	Kelch motif	0.04989	0.64369

CHAPTER 4

DISCUSSION

4.1. Heterozygous knockout of *ndr1* has no effect on sex determination

Controlled laboratory populations of zebrafish frequently exhibit a male-biased sex ratio, deviating from the expected 1:1 ratio, which has often been attributed to selective breeding and domestication of these populations [86]. The findings of this study support this trend as results indicated a male-biased sex ratio within both the mutant and WT offspring regardless of the sex of their mutant parent.

Considering the absence of significant differences in the sex ratios of offspring from *ndr1*$^{+/-}$ x WT mating pairs — regardless of which parent carried the mutation — it is difficult to extrapolate whether *ndr1* is involved in sex determination. Because the mutant fish were heterozygous, the remaining wild-type *ndr1* allele may have compensated for any potential effects of reduced *ndr1* expression. This redundancy is common in polygenic systems, where multiple genes contribute to the same process. Zebrafish lack distinct sex chromosomes and rely instead on a polygenic sex determination system, where multiple genes across different chromosomes contribute to sex determination, making the process highly sensitive to genetic variations [87]. For instance, a study utilizing a single nucleotide polymorphism array identified regions on chromosomes 5 and 16 that together accounted for approximately 16% of the variance in sex determination [88].

Another possible explanation is that even though multiple genes contribute to sex, they do not all contribute equally. Some genes, like *amh* (male-promoting) and *cyp19a1* (female-promoting), play stronger roles. Aromatase, encoded by *cyp19a1*, is an enzyme crucial for estrogen synthesis and ovarian development. Disrupting this gene leads to all-male offspring due to failed ovarian differentiation [89]. Conversely, *amh* is vital for the development of germ cells in the testis [27].

4.2. Lefty1 expression is time-dependent

The time-dependent culture experiments with Nodal treatment in zebrafish testis revealed some key observations regarding gene expression: *ndr1*, used as a positive control, did not show significant changes at any of the time points or doses tested. In contrast, *lft1* exhibited a significant increase in mRNA expression at 24 hours. The lack of significant change in *ndr1* expression could imply that the gene may not be as responsive to the rhNodal treatment in the testis as has been previously reported in the ovaries [60], or perhaps that the Nodal signaling response has reached a saturation point under the experimental conditions.

The use of *ndr1* as a positive control was based on prior knowledge about Nodal's ability to regulate its own expression via positive feedback. The lack of *ndr1* response to Nodal treatment could be explained by *lft1* expression. The observed upregulation of *lft1* mRNA expression at 24 hours following Nodal treatment aligns with the established role of Lefty proteins as feedback inhibitors of Nodal signaling, which would explain why *ndr1* expression did not significantly increase as expected. However, a Lefty response was only observed in *lft1*, which encodes Lefty1 (orthologous to Lefty1 in humans), and that too after 24 hours of culture, not earlier, which may be due to the time it takes for signaling cascades to occur. A study suggests that Lefty plays a crucial role in regulating Nodal signaling by preventing its overactivation during embryonic development [82], a mechanism likely applicable to the testis where Nodal is involved in cellular differentiation and tissue development [64,66]. In the testis, a delayed Lefty response to Nodal signaling may be necessary to fine-tune this regulation, preventing excessive signaling while maintaining proper gonadal function and fertility.

Another possible explanation for the lack of *ndr1* response could be that downstream signaling in the testis is mediated through non-canonical pathways like p38 MAPK or MEK/ERK, which have been implicated in testis development and function. According to studies conducted on mouse testis, MAPK signaling is essential for the regulation of testis development. For example, p38 MAPK signaling is required for the fate determination of Sertoli cells and primordial germ cells [90], while the MEK/ERK pathway is essential for maintaining Leydig cells in adult testis, with deficiencies of MEK1/2 resulting in underdeveloped testis, low androgen levels, and reduced fertility [91]. Another study demonstrated that p38 MAPK is essential for anterior-posterior axis specification during mouse embryo development via crosstalk between Nodal/Activin signaling; Nodal activated p38, which in turn enhanced Smad2 phosphorylation and reinforced Nodal signaling to ensure proper embryonic patterning [92]. Given the established crosstalk between Nodal and MAPK pathways in embryonic development, it is plausible that a similar interaction occurs in the testis, but further investigation is required to understand the specific molecular mechanisms that govern Nodal signaling in zebrafish testis.

It is important to note that the testis tissue is a highly heterogeneous population, composed of various cell types, including Sertoli cells, Leydig cells, germ cells, and endothelial cells, each with distinct roles in gonadal function [93]. Because of this, the observed changes in gene expression may be specific to certain cell populations. The effects of Nodal treatment on *lft1* expression, for example, could vary between different cell types within the testis. As such, the changes observed in gene expression might not be reflective of the entire tissue, but rather specific cell populations that are more sensitive to Nodal signaling.

4.3. Transcriptional responses to Nodal treatment in zebrafish testis

Differential gene expression analysis revealed a relatively small number of significantly altered genes. Such limited transcriptional change is not unexpected given that Nodal signaling is often transient and post-transcriptionally regulated, and because bulk tissue analyses may dilute cell-type–specific effects. Nonetheless, several genes of interest showed changes that suggest biologically meaningful alterations in spermatogenic processes and cellular signaling balance. Please note that the differential expression of these genes has not been independently verified; however, these results provide a useful starting point for more detailed investigation. Further research will be needed to clarify their specific roles in the testis and to determine how, or if, Nodal signaling regulates their activity.

4.3.1. Protein homeostasis and translational regulation

Among the most notable changes reported by RNA-seq was the upregulation of *klhl10b.2*, a homolog of the mammalian Kelch-like 10 (KLHL10) gene, in the Nodal-treated testis. *KLHL10* encodes a BTB/POZ domain-containing protein that interacts with ubiquitin ligase complexes, which mediate targeted protein degradation during spermatid maturation. In the testis, KLHL10 is expressed in the cytoplasm of late-stage spermatids and loss-of-function mutations or haploinsufficiency of the gene have been reported to cause male infertility in mice due to defective sperm development [73]. Their function is essential for maintaining protein quality control and facilitating the extensive cellular remodeling that occurs during late spermatogenesis. The increased expression of *klhl10b.2* in Nodal-treated testis may therefore reflect an adaptive response to Nodal signaling, potentially enhancing protein turnover and cytoplasmic remodeling within developing spermatids. This could indicate that Nodal exposure influences molecular

processes associated with the final stages of germ cell development, even in the absence of direct upregulation of canonical Nodal pathway genes.

The upregulation of *atp1a1a.4* is also interesting. Though no direct functional studies have yet been performed in zebrafish, in rats, the ubiquitous α1 isoform (ATP1A1) has been shown to mediate ouabain-sensitive signaling in Sertoli cells, promoting cyclin D1 expression and proliferation, which supports spermatogenesis [94]. Separately, studies in bovine sperm demonstrated that ouabain-sensitive Na^+/K^+-ATPase activity, which can involve ATP1A1, triggers tyrosine phosphorylation and PKA/PKC signaling during sperm capacitation (in which sperm undergo maturation after leaving the testis), highlighting a role in preparing sperm for fertilization [74]. In transgenic mice, increasing expression of the testis-specific α4 isoform (ATP1A4) enhanced sperm motility and hyperactivation, confirming that isoform-specific Na^+/K^+-ATPases are essential for sperm function [75]. Upregulation of *atp1a1a.4* in the Nodal-treated testis may therefore reflect enhanced ion homeostasis or signaling in germ or somatic cells, suggesting potential effects on sperm maturation or testicular support, even though these functions remain to be validated in zebrafish.

The upregulation of *h1m* in Nodal-treated testis may suggest that chromatin structure is being altered in germ cells. *H1M* is a histone variant that helps package DNA and is usually found in early developmental or germline cells, including zebrafish primordial germ cells [76]. In the testis, changes in histone levels often occur as germ cells prepare for later stages of sperm development [76], when DNA becomes compacted. Therefore, higher *h1m* expression after Nodal treatment could reflect an early chromatin reorganization step, possibly helping the cells stay in a more flexible state before full condensation. Histone variants like *H1M* are known to regulate the

accessibility of DNA for transcription and respond to developmental signals [95], which may explain why its expression was affected by Nodal exposure.

4.3.2. Immune homeostasis and paracrine crosstalk

Although our data focus solely on adult zebrafish testis, the mammalian study of the chemokine system provides a useful conceptual anchor to understand the downregulation of *cxcl12a* observed here. In mice, the alternative receptor CXCR7 was shown to localize to pre-meiotic germ cells and help regulate the availability of the ligand CXCL12 in the testicular environment [77]. By analogy, the downregulation of *cxcl12a* observed may reflect altered germ cell niche signaling or diminished germ cell-somatic cell communications mediated by chemokines. This complements our findings for genes like *h1m* and *klhl10b.2*, which point toward shifts in early germ-cell states and protein-turnover machinery. Together, the downregulation of chemokine signaling (*cxcl12a*) and the upregulation of germ-cell-associated (*klhl10b.2*) and chromatin-associated (*h1m*) genes may indicate that Nodal treatment is re-programming the testicular microenvironment and germ-line cell behaviour.

Like *cxcl12a*, *lyz* was also downregulated in the Nodal-treated testis. While LYZ is classically known as an antimicrobial lysozyme, emerging evidence from mammals indicates that lysozyme-like genes can have testis-specific roles beyond innate immunity. In rats, immunization against LYZL1, LYZL4, or LYZL6 impaired sperm function and reduced fertility [79]. The rat *lyzl4* gene was also shown to be expressed in testis and epididymis, with protein localizing to germ cells [80]. Similarly, LYZL family members in yaks showed age-dependent expression associated with spermatogonial proliferation and Leydig cell development [78]. Thus, the observed downregulation of *lyz* in the

Nodal-treated testis may reflect a reduction in lysozyme-like activity within the testis microenvironment, potentially affecting germ cell support or sperm maturation rather than purely immune defense. While direct functional data for zebrafish *lyz* in testis are lacking, the mammalian literature suggests that such changes could have meaningful implications for spermatogenesis or germ cell maintenance.

By contrast, *chrna2a*, which encodes the α2 subunit of the nicotinic acetylcholine receptor (nAChR) [96], was reportedly downregulated in Nodal-treated testis. This gene also showed differential exon usage, with one exon upregulated and another downregulated, suggesting a potential shift in isoform composition. Although nAChRs are best known for their roles in neurotransmission, acetylcholine signaling also occurs in non-neuronal tissues [97]. Non-neuronal cholinergic systems are present in the testis: Sertoli cells, germ cells, and peritubular cells can produce and respond to acetylcholine [98], and nAChR subunits have also been studied in testicular cells in multiple species, such as rats, mice, and honeybees [99]. These receptors have been shown to regulate intracellular calcium and second-messenger pathways that influence cell–cell junctions, Sertoli–germ cell communication, and aspects of sperm function, such as motility and acrosome reaction (the process in which a sperm releases enzymes from its acrosome to penetrate the egg's outer layer, enabling fertilization) [98]. The downregulation of *chrna2a* likely means fewer α2-containing nAChRs are being formed or that the receptor composition is changing in a way that alters calcium flow, which could then potentially disrupt sperm development rather than a complete block in spermatogenesis. A study conducted on mouse testis found that altering nAChR activity affected sperm motility and acrosome reaction [100]. These

findings suggest that cholinergic signaling helps germ cell function, so its downregulation could disrupt this delicate balance.

The downregulation of *ptgdsb.1*, which encodes prostaglandin D_2 synthase (PGD_2S), in Nodal-treated zebrafish testis may reflect a disruption of prostaglandin D_2 (PGD_2) signaling. PTGDS is a key enzyme in the testis, responsible for generating prostaglandin D_2 (PGD_2), which has important roles in testicular development and sperm maturation. PTGDS is highly expressed in Sertoli and germ cells, and its levels increase during maturation in mammalian testis. PGD_2 produced by PTGDS is implicated in the differentiation of Sertoli cells and the regulation of the testicular environment, supporting processes vital for spermatogenesis and sperm quality. Beyond its enzymatic activity, PTGDS also functions as a lipocalin-type carrier of lipophilic molecules — such as retinoids, thyroid hormones, and fatty acids — that support spermatogenesis and sperm quality [101]. Consistent with this, in the freshwater catfish *Clarias gariepinus*, a homologous *ptgds-b* gene was found to be highly expressed in seminal vesicles and developing testis, but its expression was suppressed by thyroid hormone, gonadotropin, and estradiol treatments, indicating that it is hormonally regulated within male reproductive tissues [81]. Similarly, in zebrafish, prostaglandin signaling has been shown to influence spermatogonial dynamics, with PGE_2 acting to inhibit differentiation of spermatogonia and maintain the undifferentiated state [102]. The observed downregulation of *ptgdsb.1* following Nodal treatment may therefore indicate a shift in the testicular signaling environment, where enhanced Nodal/SMAD2-3 activity could suppress prostaglandin D_2 synthesis, potentially disrupting Sertoli–germ cell communication or the lipid transport functions essential for spermatogenic support.

In mice, Nodal is expressed in a subset of type A spermatogonia and germ cells, with its receptors (ALK4, ActR-IIB) co-expressed in the same population and functional studies have shown that Nodal activates SMAD2/3 and Oct4 to promote spermatogonial proliferation [103]. Likewise, in the human fetal testis, inhibition of Nodal/Activin signaling disrupts seminiferous cord formation, somatic cell function, and germ-cell number [66]. Together, these findings support the idea that exogenous Nodal treatment in zebrafish may interfere with comparable cell–cell signaling pathways, affecting communication between germ and somatic cells; however, the mechanisms must be studied further to draw any conclusions.

4.4. Differential exon usage

At the exon level, additional changes were observed in *klhl10b.1* (a paralog of *klhl10b.2*) and *insra* (insulin receptor a), both of which displayed increased exon usage. Alternative splicing is highly prevalent during spermatogenesis and serves as a key mechanism for producing stage-specific protein isoforms with unique functions [104]. Song et al. (2020) review that genes such as *sycp3*, *dmc1*, and *akap4* undergo alternative splicing events including exon skipping, intron retention, and alternative 3′ splice sites, which generated multiple isoforms with stage-specific roles in spermatogenesis. The exon-level changes observed in this study suggest that Nodal signaling may be involved in testicular function not only by modulating gene expression levels but also by influencing splicing decisions. Because Smad proteins have been implicated in coupling transcriptional regulation with RNA-processing machinery (e.g., processing pri-mRNA by recruiting the microprocessor complex [105]), it is plausible that transient Nodal signaling alters the recruitment of splicing factors, leading to the isoform-specific changes observed here.

4.5. Canonical nodal signaling pathway expression

Interestingly, classical components of the Nodal pathway itself — *ndr1*, *ndr2*, *lefty1/2*, Smads, and Nodal receptor genes — were all detected in the dataset but were not significantly altered by treatment. The non-significant changes in expression of *ndr1* and *lft1/2* were expected, consistent with time-course analyses after 18 hours of incubation. Notably, *ndr3* was not detected in the 9-month-old testis used for RNA-seq. This is also consistent with the age-dependent experiment, which showed that *ndr3* expression was lowest at 9 months and highest in older, 18-month-old testis. Additionally, the lack of significant changes in *ndr2* or certain receptor transcripts does not necessarily imply a lack of pathway activity. Canonical Nodal and TGF-β signaling often operate through phosphorylation and nuclear translocation of Smad2/3 proteins, processes that occur at the protein level without the need for new mRNA synthesis [42]. Consequently, signaling can be robust even when transcript levels remain static. The high baseline expression of *smad2* and type II receptors *acvr2aa/ba* observed suggests the tissue was primed for rapid response to ligands, and signaling may be modulated by post-transcriptional mechanisms rather than transcriptional induction.

Another plausible explanation for the muted transcriptional signature is functional redundancy within the TGF-β superfamily. For instance, since Activin and Nodal share overlapping receptors and Smad effectors, compensatory crosstalk can buffer transcriptional outcomes when the expression of one ligand is altered [64]. Thus, the added Nodal ligand may have acted upon an already active or saturated TGF-β signaling environment, leading to subtle transcriptional rebalancing rather than dramatic pathway activation, which would explain the lack of significant change in expression levels of genes regulated by Nodal. This interpretation also aligns with the

observation that ribosomal and translational gene sets were enriched in the pathway analyses. A recent study suggests that TGF-β family ligands can influence protein synthesis machinery rather than solely driving transcriptional changes. For example, Akker et al. (2024) demonstrated in chondrocytes that TGF-β2 exposure altered ribosome composition and increased ribosome activity, affecting translation efficiency and ribosome-associated protein synthesis without necessarily changing canonical transcriptional targets. This included modulation of ribosomal proteins and shifts in IRES-dependent versus cap-dependent translation, highlighting how TGF-β signaling can regulate protein output post-transcriptionally.

4.6. Pathway enrichment analyses

4.6.1. Baseline transcriptional activity in zebrafish testis

Functional analysis of the most highly expressed genes in control zebrafish testis revealed that protein synthesis and ribosome activity dominate the transcriptome. This was driven by genes such as *rpl3*, *rpl12*, *rpl13a*, and *rps19*, reflecting the high protein production required for spermatogenesis. Mitochondrial energy pathways, including *mt-atp6* and *atp5f1b*, were also enriched, consistent with the energetic demands of germ cells and supporting somatic cells. Additional pathways, such as Notch signaling (*uba52*, *rps27a*), ER quality control, and regulated cell death, indicate that the testis maintains ongoing control of cell fate, protein quality, and turnover. These results provide a clear baseline of the key processes active under untreated conditions, which helps interpret the modest changes seen after rhNodal treatment. The limited effect on canonical Nodal pathway genes suggests that Nodal may act subtly, in specific cell types, or through mechanisms not captured in bulk RNA-seq.

4.6.2. Translational and metabolic responses to Nodal exposure

Pathway-level analyses provide a broader perspective on transcriptional changes in the testis, especially given the relatively small number of individual DEGs. Both CAMERA and clusterProfiler highlighted enrichment of pathways related to translation, ribosomal structure, and ribonucleoprotein complex biogenesis. Notably, both methods indicated that these ribosomal and translation-related pathways were downregulated in Nodal-treated testis. These results suggest that even subtle transcriptional responses to Nodal exposure are largely focused on post-transcriptional and translational processes. The 18-hour treatment appeared to influence the biosynthetic and metabolic state of testicular cells rather than driving large-scale transcriptional reprogramming. Enrichment of ribosomal and translation-related gene sets indicates that Nodal signaling may transiently modify protein synthesis machinery in germ cells or supporting somatic cells.

This aligns with the notion that zebrafish spermatogenesis relies on robust translational activity, particularly during meiosis and spermiogenesis when extensive protein turnover and cellular remodeling occur. Single-cell transcriptome profiling of zebrafish testis has confirmed high expression of genes associated with translation and ribosome function during spermatogenesis [107], highlighting the importance of post-transcriptional control in germ cell development. Comparable observations in other systems show that TGF-β family ligands, including activin, regulate ribosome biogenesis and translational efficiency to coordinate cell growth and differentiation. For example, Martins et al. (2017) demonstrated that TGF-β/Activin signaling via Smad2 is required for ribosome assembly and cell growth in Drosophila, linking pathway activation to translational regulation. In addition, Liu & Chen (2022) reviewed that TGF-β signaling

intersects with metabolic pathways to influence translation rates and ribosome composition, which further supports the idea that post-transcriptional mechanisms are key mediators of ligand effects.

4.6.3. Reproductive pathway enrichment and zp gene expression

The enrichment of reproductive pathways such as “binding of sperm to zona pellucida” and “acrosin binding” in the Nodal-treated testis primarily reflected the upregulation of egg coat genes, including *zp3a1*, *zp3a2*, and related *zp* family members. In zebrafish, sperm do not undergo a classical acrosome reaction as in mammals; instead, fertilization occurs via the micropyle, a specialized opening in the egg envelope that allows sperm entry [15]. Therefore, the GO term “acrosin binding” should not be interpreted as evidence of a canonical acrosomal mechanism but likely represents genes involved in sperm–egg recognition and interaction. The unexpected detection — and subsequent enrichment — of these ovary-associated genes in the testis suggests that these genes are expressed outside of their classical ovary/egg envelope context. Recent single-cell RNA-seq studies revealed that *zp* gene expression in testis is confined to only subsets of germ cells, such as those in early-stage spermatogenesis (spermatogonia and spermatocytes), particularly in aged or incomplete testis [109]. In contrast, the testis used in this project were from 9-month-old, reproductively healthy males. However, due to the nature of the *ex vivo* testis culture used in this project, it is unclear which cell types within the testis exhibited an increase in *zp* genes post-Nodal treatment. Perhaps transient Nodal exposure may have induced a transcriptional state resembling that of stressed or partially dedifferentiated germ cells, consistent with Nodal’s known roles in regulating pluripotency and germ cell fate [63]. This raises the possibility that Nodal signaling can influence germline gene expression beyond its

developmental functions, perhaps by altering the balance between differentiation and maintenance programs within the testis.

4.6.4. Immune and paracrine signaling modulation by Nodal

Enrichment of immune-related pathways was also observed, which included GO terms such as immune effector processes, defense response to bacteria, and response to stress, all of which appeared to be downregulated in the Nodal-treated samples. The testis is known to be an immune-privileged organ, where immune activity is tightly regulated to protect developing germ cells while preserving the ability to respond to infection or injury. This balance is maintained by local immune cells and somatic cells, particularly Sertoli cells, which produce and secrete cytokines, including TGF-β and Activin A [110,111]. Given that Nodal, Activin, and other TGF-β ligands share Smad2/3 signaling pathways, exogenous Nodal might have changed paracrine signaling dynamics among germ and somatic cells in the testis.

Supporting this idea, specific immune-related genes such as *lyz* and *pglyrp6* were significantly downregulated in Nodal-treated testis. In zebrafish, *pglyrp6* encodes a peptidoglycan recognition protein that is expressed in immune tissues and upregulated in response to bacterial challenge. While its function in the testis has not been characterized, and there is no evidence that Nodal directly regulates immunity, the observed down-regulation may reflect indirect effects: deviations in paracrine signaling networks among Sertoli, germ, and somatic cells could lead to transcriptional adjustments by innate immune genes. The broader literature on TGF-β superfamily signaling reinforces this view; TGF-β ligands, through Smad2/3-dependent pathways, are known to regulate immune cell development, differentiation, and homeostasis, often

dampening immune responses in tissues [112]. The observed immune pathway enrichment and downregulation of specific innate immune genes could reflect both direct Nodal effects and compensatory responses from other TGF-β family members stepping in to maintain balance.

CHAPTER 5

SUMMARY & FUTURE DIRECTIONS

This project aimed to investigate the role of Nodal in zebrafish gonadal function, with a particular focus on its involvement in sex determination and testis function. This study found that *ndr1* heterozygosity did not significantly affect sex ratio. *Ex vivo* treatment with rhNodal resulted in a time-dependent upregulation of *lft1*, while canonical Nodal pathway components, including *ndr1*, showed minimal transcriptional changes. This suggests that the testis may be primed for Nodal signaling, with activity regulated post-transcriptionally or through feedback inhibition rather than transcriptional induction. It is also worth noting that rhNodal may be less potent in its effects compared to the endogenous *ndr* genes, which is why our lab has been working on creating inducible *ndr* knockout lines that would allow knockouts after crucial embryo stages to provide viable homozygous mutant adults.

Differential gene expression analyses revealed modest but notable changes, including the upregulation of *klhl10b.2* and *h1m* in Nodal-treated testis, indicating potential effects on protein turnover, chromatin reorganization, and late-stage spermatid development. Conversely, downregulation of *chrna2a* suggests altered cholinergic signaling in germ or somatic cells, which could impact calcium-mediated cell interactions. Exon-level analyses revealed alternative splicing events in genes such as *klhl10b.1* and *insra*, which is consistent with the role of Smad-dependent signaling in regulating RNA processing. Pathway-level analyses highlighted translational and ribosomal processes, as well as reproductive and immune-related pathways, suggesting that Nodal exposure may subtly modulate protein synthesis, germ cell preparation, and local immune signaling in the testis. These findings highlight a potential role for Nodal signaling in zebrafish testicular function that differs from its previously characterized effects in ovarian cells.

However, these conclusions are limited by several factors. Using bulk RNA-seq from a single age group (9-month-old testis) and a single treatment time point may have obscured cell-type-specific or age-dependent responses. Additionally, *ndr3* was not expressed at this stage, and the observed DEGs and splicing changes were not experimentally validated. Future studies should incorporate single-cell transcriptomics, multiple developmental stages, and protein-level validation to clarify how Nodal signaling affects specific testicular cell populations. It would also be beneficial to determine whether effects are mediated through Lefty1 or alternative pathways, and establish the functional consequences of these transcriptional changes. Together, these approaches would provide a more robust understanding of Nodal's role in testis function.

This research is important because it begins to explore the largely uncharacterized role of Nodal signaling in the adult zebrafish testis, a system previously studied in embryogenesis and ovarian function. Although the study did not definitively reveal the precise mechanism of Nodal action in testicular cells, the observed transcriptional and splicing changes — particularly in *lft1*, translational machinery, and immune-related pathways — provide preliminary evidence that Nodal may influence germ cell development, protein synthesis, and local paracrine signaling. These findings highlight potential points of crosstalk between Smad2/3-dependent signaling and somatic-germ cell interactions, suggesting a broader role for TGF-β family ligands in testis physiology. Despite not fully elucidating the mechanism, this study establishes a foundation for future work to dissect Nodal's functions, identify specific responsive cell populations, and clarify its interactions with other TGF-β family members.

REFERENCES

1. Howe, K. *et al.* The zebrafish reference genome sequence and its relationship to the human genome. *Nature 2013 496:7446* 496, 498–503 (2013).
2. Veldman, M. B. & Lin, S. Zebrafish as a Developmental Model Organism for Pediatric Research. *Pediatric Research 2008 64:5* 64, 470–476 (2008).
3. Choi, T. Y., Choi, T. I., Lee, Y. R., Choe, S. K. & Kim, C. H. Zebrafish as an animal model for biomedical research. *Experimental & Molecular Medicine 2021 53:3* 53, 310–317 (2021).
4. Kimura, Y., Hisano, Y., Kawahara, A. & Higashijima, S. I. Efficient generation of knock-in transgenic zebrafish carrying reporter/driver genes by CRISPR/Cas9-mediated genome engineering. *Scientific Reports 2014 4:1* 4, 1–7 (2014).
5. Angom, R. S. & Nakka, N. M. R. Zebrafish as a Model for Cardiovascular and Metabolic Disease: The Future of Precision Medicine. *Biomedicines 2024, Vol. 12, Page 693* 12, 693 (2024).
6. Doyle, J. M. & Croll, R. P. A Critical Review of Zebrafish Models of Parkinson's Disease. *Front Pharmacol* 13, (2022).
7. Aharon, D. & Marlow, F. L. Sexual determination in zebrafish. *Cell Mol Life Sci* 79, 8 (2021).
8. Dai, X., Jin, X., Chen, X., He, J. & Yin, Z. Sufficient Numbers of Early Germ Cells Are Essential for Female Sex Development in Zebrafish. *PLoS One* 10, e0117824 (2015).
9. King, A. C., Gut, M. & Zenker, A. K. Shedding new light on early sex determination in zebrafish. *Archives of Toxicology 2020 94:12* 94, 4143–4158 (2020).
10. Ruan, Y. *et al.* New insights into the all-testis differentiation in zebrafish with compromised endogenous androgen and estrogen synthesis. *PLoS Genet* 20, e1011170 (2024).
11. Ye, M. & Chen, Y. Zebrafish as an emerging model to study gonad development. *Comput Struct Biotechnol J* 18, 2373 (2020).
12. Dranow, D. B. *et al.* Bmp15 Is an Oocyte-Produced Signal Required for Maintenance of the Adult Female Sexual Phenotype in Zebrafish. *PLoS Genet* 12, e1006323 (2016).
13. Wittkopp, N., Domingues, A. M. de J. & Ketting, R. F. miR214 regulates sex determination through gsdf in zebrafish. *bioRxiv* 2024.05.01.592007 (2024) doi:10.1101/2024.05.01.592007.
14. Hoo, J. Y., Kumari, Y., Shaikh, M. F., Hue, S. M. & Goh, B. H. Zebrafish: A Versatile Animal Model for Fertility Research. *Biomed Res Int* 2016, 9732780 (2016).
15. Yi, X. *et al.* The effector of Hippo signaling, Taz, is required for formation of the micropyle and fertilization in zebrafish. *PLoS Genet* 15, e1007408 (2019).
16. Fissore, R. A., Lopes, E. M. & Carpentiero, F. Zebrafish sperm outsource activation to eggs' protease-activated receptors. *PLoS Biol* 23, e3003214 (2025).
17. García-Castro, P., Giambó-Falian, I., Carvacho, I. & Fuentes, R. Phenogenetics of cortical granule dynamics during zebrafish oocyte-to-embryo transition. *Front Cell Dev Biol* 13, 1514461 (2025).

18. Schulz, R. W. *et al.* Endocrine and paracrine regulation of zebrafish spermatogenesis: the Sertoli cell perspective. *Animal Reproduction (AR)* 12, 81–87 (2018).

19. Leal, M. C. *et al.* Histological and Stereological Evaluation of Zebrafish (Danio rerio) Spermatogenesis with an Emphasis on Spermatogonial Generations. *Biol Reprod* 81, 177–187 (2009).

20. Ye, M. & Chen, Y. Zebrafish as an emerging model to study gonad development. *Comput Struct Biotechnol J* 18, 2373–2380 (2020).

21. Zhai, G. *et al.* Characterization of Sexual Trait Development in cyp17a1-Deficient Zebrafish. *Endocrinology* 159, 3549–3562 (2018).

22. Crespo, D. *et al.* Insulin-like 3 affects zebrafish spermatogenic cells directly and via Sertoli cells. *Communications Biology 2021 4:1* 4, 1–13 (2021).

23. Nóbrega, R. H. *et al.* Spermatogonial Stem Cell Niche and Spermatogonial Stem Cell Transplantation in Zebrafish. *PLoS One* 5, e12808 (2010).

24. de Waal, P. P., Wang, D. S., Nijenhuis, W. A., Schulz, R. W. & Bogerd, J. Functional characterization and expression analysis of the androgen receptor in zebrafish (Danio rerio) testis. *Reproduction* 136, 225–234 (2008).

25. Gautier, A., Sohm, F., Joly, J. S., Le Gac, F. & Lareyre, J. J. The Proximal Promoter Region of the Zebrafish gsdf Gene Is Sufficient to Mimic the Spatio-Temporal Expression Pattern of the Endogenous Gene in Sertoli and Granulosa Cells. *Biol Reprod* 85, 1240–1251 (2011).

26. Zhao, C. *et al.* Genetic analysis of activin/inhibin β subunits in zebrafish development and reproduction. *PLoS Genet* 18, (2022).

27. Yan, Y. L. *et al.* A Hormone That Lost Its Receptor: Anti-Müllerian Hormone (AMH) in Zebrafish Gonad Development and Sex Determination. *Genetics* 213, 529 (2019).

28. Yamamoto, Y., Hishikawa, D. & Ono, F. Trpv4-mediated apoptosis of Leydig cells induced by high temperature regulates sperm development and motility in zebrafish. *Commun Biol* 7, 96 (2024).

29. Xie, Y. *et al.* The highly overlapping actions of Lh signaling and Fsh signaling on zebrafish spermatogenesis. *J Endocrinol* 234, 233–246 (2017).

30. Crespo, D. *et al.* Endocrine and local signaling interact to regulate spermatogenesis in zebrafish: Follicle-stimulating hormone, retinoic acid and androgens. *Development (Cambridge)* 146, (2019).

31. Zhang, Q. *et al.* Zebrafish cyp11c1 Knockout Reveals the Roles of 11-ketotestosterone and Cortisol in Sexual Development and Reproduction. *Endocrinology* 161, (2020).

32. Alsop, D. & Vijayan, M. M. Molecular programming of the corticosteroid stress axis during zebrafish development. *Comp Biochem Physiol A Mol Integr Physiol* 153, 49–54 (2009).

33. Tovo-Neto, A. *et al.* Cortisol Directly Stimulates Spermatogonial Differentiation, Meiosis, and Spermiogenesis in Zebrafish (Danio rerio) Testicular Explants. *Biomolecules* 10, 429 (2020).

34. Fuzzen, M. L. M., Bernier, N. J. & Van Der Kraak, G. Differential effects of 17β-estradiol and 11-ketotestosterone on the endocrine stress response in zebrafish (Danio rerio). *Gen Comp Endocrinol* 170, 365–373 (2011).

35. Clelland, E. S., Tan, Q., Balofsky, A., Lacivita, R. & Peng, C. Inhibition of premature oocyte maturation: A role for bone morphogenetic protein 15 in zebrafish ovarian follicles. *Endocrinology* 148, 5451–5458 (2007).

36. Wu, T. *et al.* Activin, Inhibin, and Follistatin in Zebrafish Ovary: Expression and Role in Oocyte Maturation 1. *Biol Reprod* 62, 1585–1592 (2000).

37. Chea, H. K., Wright, C. V. & Swalla, B. J. Nodal signaling and the evolution of deuterostome gastrulation. *Dev Dyn* 234, 269–278 (2005).

38. Mendis, S. H. S., Meachem, S. J., Sarraj, M. A. & Loveland, K. L. Activin A balances Sertoli and germ cell proliferation in the fetal mouse testis. *Biol Reprod* 84, 379–391 (2011).

39. Poon, S. K., So, W. K., Yu, X., Liu, L. & Ge, W. Characterization of inhibin α subunit (inha) in the zebrafish: evidence for a potential feedback loop between the pituitary and ovary. *Reproduction* 138, 709–719 (2009).

40. Garrel, G. *et al.* Anti-Müllerian hormone: a new actor of sexual dimorphism in pituitary gonadotrope activity before puberty. *Scientific Reports 2016 6:1* 6, 1–11 (2016).

41. Li, X. *et al.* Bone morphogenetic protein 4 inhibits rat stem/progenitor Leydig cell development and regeneration via SMAD-dependent and SMAD-independent signaling. *Cell Death Dis* 13, 1039 (2022).

42. Nakashima, H. *et al.* Canonical TGF-Signaling Negatively Regulates Neuronal Morphogenesis through TGIF/Smad Complex-Mediated CRMP2 Suppression. *J Neurosci.* 38, 4791–4810 (2018).

43. Tan, Q., Balofsky, A., Weisz, K. & Peng, C. Role of activin, transforming growth factor-β and bone morphogenetic protein 15 in regulating zebrafi sh oocyte maturation ☆. *Comparative Biochemistry and Physiology, Part A* 153, 18–23 (2008).

44. Engel, M. E., McDonnell, M. A., Law, B. K. & Moses, H. L. Interdependent SMAD and JNK signaling in transforming growth factor-beta-mediated transcription. *J Biol Chem* 274, 37413–37420 (1999).

45. Bakin, A. V., Tomlinson, A. K., Bhowmick, N. A., Moses, H. L. & Arteaga, C. L. Phosphatidylinositol 3-kinase function is required for transforming growth factor beta-mediated epithelial to mesenchymal transition and cell migration. *J Biol Chem* 275, 36803–36810 (2000).

46. Dougan, S. T., Warga, R. M., Kene, D. A., Schier, A. F. & Talbot, W. S. The role of the zebrafish nodal-related genes squint and cyclops in patterning of mesendoderm. *Development* 130, 1837–1851 (2003).

47. Montague, T. G., Gagnon, J. A. & Schier, A. F. Conserved regulation of Nodal-mediated left-right patterning in zebrafish and mouse. *Development* 145, (2018).

48. Quail, D. F., Siegers, G. M., Jewer, M. & Postovit, L.-M. Nodal signalling in embryogenesis and tumourigenesis. *Int J Biochem Cell Biol* 45, 885–898 (2013).

49. Zinski, J., Tajer, B. & Mullins, M. C. TGF-β Family Signaling in Early Vertebrate Development. *Cold Spring Harb Perspect Biol* 10, (2018).

50. Long, S., Ahmad, N. & Rebagliati, M. The zebrafish nodal-related gene southpaw is required for visceral and diencephalic left-right asymmetry. *Development* 130, 2303–2316 (2003).

51. Aquilina-Beck, A., Ilagan, K., Liu, Q. & Liang, J. O. Nodal signaling is required for closure of the anterior neural tube in zebrafish. *BMC Dev Biol* 7, (2007).

52. Fan, X. *et al.* Nodal signals mediate interactions between the extra-embryonic and embryonic tissues in zebrafish. *Dev Biol* 310, 363–378 (2007).

53. Kurup, A. J., Bailet, F. & Fürthauer, M. Myosin1G promotes Nodal signaling to control zebrafish left-right asymmetry. *Nature Communications 2024 15:1* 15, 1–19 (2024).

54. Xing, C. *et al.* Maternal Factors and Nodal Autoregulation Orchestrate Nodal Gene Expression for Embryonic Mesendoderm Induction in the Zebrafish. *Front Cell Dev Biol* 10, 887987 (2022).

55. Yan, Y.-T. *et al.* Dual Roles of Cripto as a Ligand and Coreceptor in the Nodal Signaling Pathway. *Mol Cell Biol* 22, 4439 (2002).

56. Gritsman, K. *et al.* The EGF-CFC protein one-eyed pinhead is essential for nodal signaling. *Cell* 97, 121–132 (1999).

57. Chen, C. & Shen, M. M. Two modes by which lefty proteins inhibit nodal signaling. *Current Biology* 14, 618–624 (2004).

58. Park, C. B., Demayo, F. J., Lydon, J. P. & Dufort, D. NODAL in the Uterus Is Necessary for Proper Placental Development and Maintenance of Pregnancy 1. *Biol Reprod* 86, 194–195 (2012).

59. Ayash, T. A., Starr, L. M. & Dufort, D. Nodal is required to maintain the uterine environment in an anti-inflammatory state during pregnancy †. *Biol Reprod* 102, 1340–1350 (2020).

60. Zayed, Y., Malik, R., Qi, X. & Peng, C. Nodal regulates ovarian functions in zebrafish. *Mol Cell Endocrinol* 511, (2020).

61. Spiller, C. M., Bowles, J. & Koopman, P. Nodal/Cripto signaling in fetal male germ cell development: implications for testicular germ cell tumors. *Int J Dev Biol* 57, 211–219 (2013).

62. Souquet, B. *et al.* Nodal Signaling Regulates the Entry into Meiosis in Fetal Germ Cells. *Endocrinology* 153, 2466–2473 (2012).

63. Spiller, C. M. *et al.* Endogenous Nodal signaling regulates germ cell potency during mammalian testis development. *Development* 139, 4123–4132 (2012).

64. Poulsen, K. H. & Jørgensen, A. Role of Nodal signalling in testis development and initiation of testicular cancer. *Reproduction* 158, R67–R77 (2019).

65. Spiller, C., Burnet, G. & Bowles, J. Regulation of fetal male germ cell development by members of the TGFβ superfamily. *Stem Cell Res* 24, 174–180 (2017).

66. Jørgensen, A. *et al.* Nodal Signaling Regulates Germ Cell Development and Establishment of Seminiferous Cords in the Human Fetal Testis. *Cell Rep* 25, 1924-1937.e4 (2018).

67. Leal, M. C. *et al.* Zebrafish primary testis tissue culture: An approach to study testis function ex vivo. *Gen Comp Endocrinol* 162, 134–138 (2009).

68. Kolberg, L. *et al.* g:Profiler—interoperable web service for functional enrichment analysis and gene identifier mapping (2023 update). *Nucleic Acids Res* 51, W207–W212 (2023).

69. Yu, G., Wang, L. G., Han, Y. & He, Q. Y. clusterProfiler: an R Package for Comparing Biological Themes Among Gene Clusters. *https://home.liebertpub.com/omi* 16, 284–287 (2012).

70. Wu, D. & Smyth, G. K. Camera: a competitive gene set test accounting for inter-gene correlation. *Nucleic Acids Res* 40, (2012).

71. Anders, S., Reyes, A. & Huber, W. Detecting differential usage of exons from RNA-seq data. *Genome Res* 22, 2008–2017 (2012).

72. Wu, Y. L. & Gong, Z. A novel zebrafish kelchlike gene klhl and its human ortholog KLHL display conserved expression patterns in skeletal and cardiac muscles. *Gene* 338, 75–83 (2004).

73. Yan, W., Ma, L., Burns, K. H. & Matzuk, M. M. Haploinsufficiency of kelch-like protein homolog 10 causes infertility in male mice. *Proc Natl Acad Sci U S A* 101, 7793 (2004).

74. Newton, L. D. *et al.* Na+/K+ATPase regulates sperm capacitation through a mechanism involving kinases and redistribution of its testis-specific isoform. *Mol Reprod Dev* 77, 136–148 (2010).

75. Jimenez, T. *et al.* Increased expression of the Na,K-ATPase alpha4 isoform enhances sperm motility in transgenic mice. *Biol Reprod* 84, 153–161 (2011).

76. Müller, K., Thisse, C., Thisse, B. & Raz, E. Expression of a linker histone-like gene in the primordial germ cells in zebrafish. *Mech Dev* 117, 253–257 (2002).

77. Westernströer, B. *et al.* Profiling of Cxcl12 receptors, Cxcr4 and Cxcr7 in murine testis development and a spermatogenic depletion model indicates a role for Cxcr7 in controlling Cxcl12 activity. *PLoS One* 9, (2014).

78. La, Y. *et al.* Age-dependent changes in the expression and localization of LYZL4, LYZL6 and PCNA during testicular development in the Ashidan yak. *Anim Biotechnol* 35, (2024).

79. Narmadha, G. & Yenugu, S. Immunization against lysozyme-like proteins affect sperm function and fertility in the rat. *J Reprod Immunol* 118, 100–108 (2016).

80. Narmadha, G., Muneswararao, K., Rajesh, A. & Yenugu, S. Characterization of a novel lysozyme-like 4 gene in the rat. *PLoS One* 6, (2011).

81. Gunti, S., Ayinampudi, P., Chenichery, S., Aparna, D. G. & Balasubramanian, S. Modulation of lipocalin-type prostaglandin D2 synthase expression in catfish seminal vesicles by thyroid disrupting agents and hormones. *Comparative Biochemistry and Physiology - C Toxicology and Pharmacology* 158, 199–206 (2013).

82. Rogers, K. W. *et al.* Nodal patterning without Lefty inhibitory feedback is functional but fragile. *Elife* 6, e28785 (2017).

83. Aykul, S., Ni, W., Mutatu, W. & Martinez-Hackert, E. Human Cerberus Prevents Nodal-Receptor Binding, Inhibits Nodal Signaling, and Suppresses Nodal-Mediated Phenotypes. *PLoS One* 10, e0114954 (2015).

84. Izzi, L. *et al.* Foxh1 recruits Gsc to negatively regulate Mixl1 expression during early mouse development. *EMBO J* 26, 3132 (2007).

85. Gordillo, M., Wu, R., Banks, K. M., Silva, N. de & Evans, T. GATA6 Mediates Endoderm and Mesoderm Progenitor Fate Driven by WNT and NODAL Signaling. *bioRxiv* 2025.06.20.660704 (2025) doi:10.1101/2025.06.20.660704.

86. Hosseini, S. *et al.* Genetic mechanism underlying sexual plasticity and its association with colour patterning in zebrafish (Danio rerio). *BMC Genomics* 20, 1–17 (2019).

87. Liew, W. C. *et al.* Polygenic Sex Determination System in Zebrafish. *PLoS One* 7, e34397 (2012).

88. Bradley, K. M. *et al.* An SNP-Based Linkage Map for Zebrafish Reveals Sex Determination Loci. *G3 Genes|Genomes|Genetics* 1, 3–9 (2011).

89. Lau, E. S. W., Zhang, Z., Qin, M. & Ge, W. Knockout of Zebrafish Ovarian Aromatase Gene (cyp19a1a) by TALEN and CRISPR/Cas9 Leads to All-male Offspring Due to Failed Ovarian Differentiation. *Scientific Reports 2016 6:1* 6, 1–14 (2016).

90. Luo, D., He, Z., Yu, C. & Guan, Q. Role of p38 MAPK Signalling in Testis Development and Male Fertility. *Oxid Med Cell Longev* 2022, 6891897 (2022).

91. Yamashita, S., Tai, P., Charron, J., Ko, C. M. & Ascoli, M. The Leydig Cell MEK/ERK Pathway Is Critical for Maintaining a Functional Population of Adult Leydig Cells and for Fertility. *Molecular Endocrinology* 25, 1211 (2011).

92. Clements, M., Pernaute, B., Vella, F. & Rodriguez, T. A. Crosstalk between Nodal/Activin and MAPK p38 Signaling Is Essential for Anterior-Posterior Axis Specification. *Current Biology* 21, 1289–1295 (2011).

93. Qian, P., Kang, J., Liu, D. & Xie, G. Single Cell Transcriptome Sequencing of Zebrafish Testis Revealed Novel Spermatogenesis Marker Genes and Stronger Leydig-Germ Cell Paracrine Interactions. *Front Genet* 13, 851719 (2022).

94. Lucas, T. F. G., Amaral, L. S., Porto, C. S. & Quintas, L. E. M. Na+/K+-ATPase α1 isoform mediates ouabain-induced expression of cyclin D1 and proliferation of rat sertoli cells. *Reproduction* 144, 737–745 (2012).

95. Pan, C. & Fan, Y. Role of H1 Linker Histones in Mammalian Development and Stem Cell Differentiation. *Biochim Biophys Acta* 1859, 496 (2015).

96. Zoli, M., Pucci, S., Vilella, A. & Gotti, C. Neuronal and Extraneuronal Nicotinic Acetylcholine Receptors. *Curr Neuropharmacol* 16, 338 (2018).

97. Barbagallo, F., Assenza, M. R., Torrisi, F., Buonacquisto, A. & Pallotti, F. The Smoky Impact of Nicotinic Acetylcholine Receptors on Testicular Function. *J Clin Med* 13, 5097 (2024).

98. Schirmer, S. U. *et al.* The cholinergic system in rat testis is of non-neuronal origin. *Reproduction* 142, 157–166 (2011).

99. Wessler, I. K. & Kirkpatrick, C. J. Non-neuronal acetylcholine involved in reproduction in mammals and honeybees. *J Neurochem* 142, 144–150 (2017).

100. Makino, Y., Hiradate, Y., Umezu, K., Hara, K. & Tanemura, K. Expression and Possible Role of Nicotinic Acetylcholine Receptor ε Subunit (AChRe) in Mouse Sperm. *Biology 2021, Vol. 10, Page 46* 10, 46 (2021).

101. Rossitto, M., Ujjan, S., Poulat, F. & Boizet-Bonhoure, B. Multiple roles of the prostaglandin D2 signaling pathway in reproduction. *Reproduction* 149, R49–R58 (2015).

102. Crespo, D. *et al.* PGE2 inhibits spermatogonia differentiation in zebrafish: interaction with Fsh and an androgen. *Journal of Endocrinology* 244, 163–175 (2020).

103. Zuping, H., Jiji, J., Kokkinaki, M. & Dym, M. Nodal signaling via an autocrine pathway promotes proliferation of mouse spermatogonial stem/progenitor cells through Smad2/3 and Oct-4 activation. *Stem Cells* 27, 2580–2590 (2009).

104. Song, H., Wang, L., Chen, D. & Li, F. The Function of Pre-mRNA Alternative Splicing in Mammal Spermatogenesis. *Int J Biol Sci* 16, 38 (2020).

105. Davis, B. N., Hilyard, A. C., Lagna, G. & Hata, A. SMAD proteins control DROSHA-mediated microRNA maturation. *Nature 2008 454:7200* 454, 56–61 (2008).

106. van den Akker, G. G. H. *et al.* TGF-β2 Induces Ribosome Activity, Alters Ribosome Composition and Inhibits IRES-Mediated Translation in Chondrocytes. *Int J Mol Sci* 25, 5031 (2024).

107. Qian, P., Kang, J., Liu, D. & Xie, G. Single Cell Transcriptome Sequencing of Zebrafish Testis Revealed Novel Spermatogenesis Marker Genes and Stronger Leydig-Germ Cell Paracrine Interactions. *Front Genet* 13, 851719 (2022).

108. Liu, H. & Chen, Y. G. The Interplay Between TGF-β Signaling and Cell Metabolism. *Front Cell Dev Biol* 10, 846723 (2022).

109. Sposato, A. L. *et al.* Germ cell progression through zebrafish spermatogenesis declines with age. *Development* 151, dev204319 (2024).

110. Meinhardt, A. & Hedger, M. P. Immunological, paracrine and endocrine aspects of testicular immune privilege. *Mol Cell Endocrinol* 335, 60–68 (2011).

111. Washburn, R. L. & Dufour, J. M. Complementing Testicular Immune Regulation: The Relationship between Sertoli Cells, Complement, and the Immune Response. *Int J Mol Sci* 24, 3371 (2023).

112. Chen, B., Mu, C., Zhang, Z., He, X. & Liu, X. The Love-Hate Relationship Between TGF-β Signaling and the Immune System During Development and Tumorigenesis. *Front Immunol* 13, 891268 (2022).

APPENDICES

APPENDIX A — Supplemental Figures and Tables

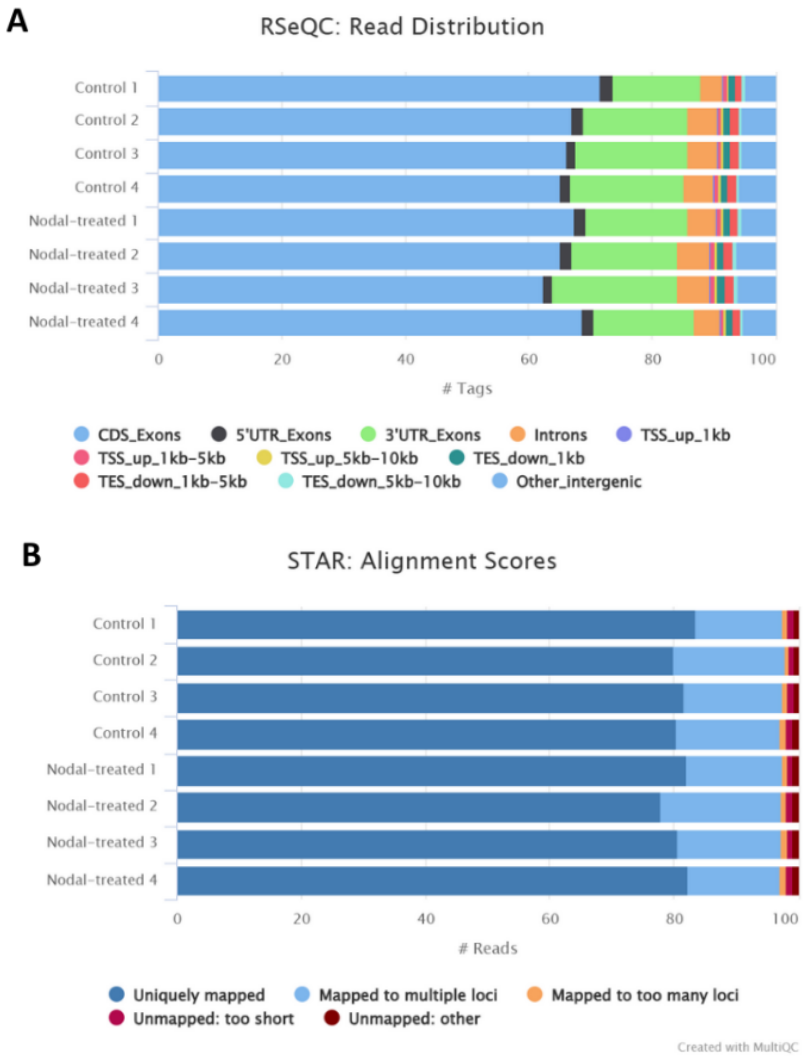

Figure A1: RNA-seq quality control metrics. Summary plots showing (A) the distribution of reads across genomic features as assessed by RSeQC, and (B) alignment statistics generated by the STAR aligner. The read distribution indicates that the majority of reads map to exonic regions, consistent with successful mRNA library preparation. STAR alignment metrics show high overall mapping rates for all samples. The complete MultiQC report for all samples is available upon request.

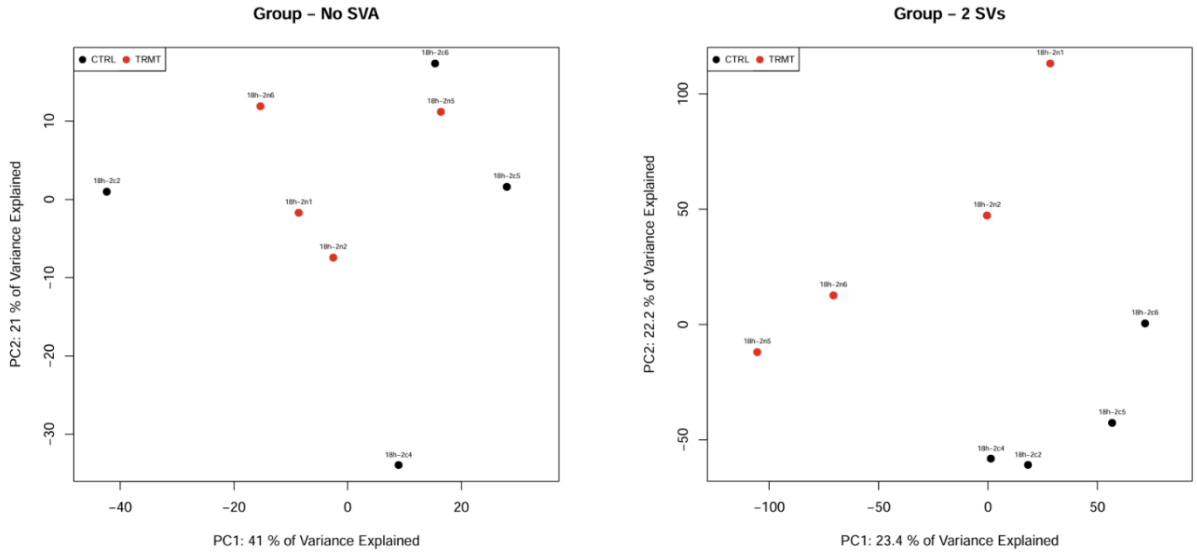

Figure A2: RNA-seq sample clustering before and after surrogate variable analysis. PCA showing the clustering of RNA-seq samples based on normalized counts before and after including two surrogate variables (SVs) identified by SVA. Incorporating SVs reduced unwanted variation and improved sample grouping for downstream differential expression analysis.